



Suez University
Faculty of Petroleum and Mining Engineering
Engineering Science Department



STUDY OF SOLAR BRACKISH WATER DESALINATION FOR DOMESTIC APPLICATIONS

A Thesis
Submitted in Fulfillment of the Requirements
For the Degree of M. Sc. In Energy Engineering

By

Eng. Mohamed Abdel Fattah Aboel Magd

B. Sc. Mechanical Engineering - Military Technical College

2007

Supervision Committee

Dr. Hussein M. Soliman

Solar Energy Department
National Research Centre
Giza, Egypt

Dr. Hani M. El Gohary

Engineering Sc. Department
Faculty of Petroleum and Mining Engineering
Suez University, Egypt

**Suez
2016**



Suez University
Faculty of Petroleum and Mining Engineering
Engineering Science Department



STUDY OF SOLAR BRACKISH WATER DESALINATION FOR DOMESTIC APPLICATIONS

A Thesis
Submitted in Fulfillment of the Requirements
For the Degree of M. Sc. In Energy Engineering

By

Eng. Mohamed Abdel Fattah AboelMagd

B. Sc. Mechanical Engineering - Military Technical College
2007

Approval Committee

Prof. Dr. Sameh A. Nada

Professor of Mechanical Engineering
Dean for Faculty of Engineering
Banha University, Egypt

Dr. Hussein M. Soliman

Solar Energy Department
National Research Centre
Giza, Egypt

Dr. Ahmed S. Mohamed

Engineering Sc. Department
Faculty of Petroleum and Mining Engineering
Suez University, Egypt

Dr. Hani M. EL Gohary

Engineering Sc. Department
Faculty of Petroleum and Mining Engineering
Suez University, Egypt

**Suez
2016**

ACKNOWLEDGMENT

First of all, I thank **ALLAH** the merciful, for helping me to complete this work, and I hope this work be useful to my country Egypt.

Thanks a lot to...

Dr. Hussein Mohamed Soliman, National Research Center, for offering all helps for the fulfillment of this work.

Dr. Hani Elgohary, Engineering Science Department, for his supreme supervising and his support to the fulfillment of this work.

Dr. Mohamed Abdel WahabSharafEldean, Engineering Science Department, for giving a great opportunity to learn from his experience in this field.

My wife, for helping me to complete this work

Mohamed Abdel Fattah AboelMagd

June 2015

ABSTRACT

Many remote areas of the world such as coastal desert areas in the Middle East and some Mediterranean are suffering from a severe shortage of drinking water. Egypt, whose population about 90 million will face serious water shortages by 2025. Exploitation of natural fresh water resources combined with higher water demand has led to increasing the demand for alternative fresh water resources.

Solar water distillation has been a subject of great interest for several decades. Solar desalination techniques are considered to be clean operations for producing clean water from the saline water. Egypt is considered to be one of the high insolation countries of the world. Suez-Gulf region is considered to be one of the highest insolation regions in Egypt. It is very important to utilize this solar energy in Egypt (Suez-Gulf) in desalination technologies (small and large sizes).

In the present work, a small size of a solar still distillation unit coupled with different types of low concentration ratios of solar water heater (i.e. Flat plate solar water heater and evacuated tube solar water heater) has been designed and tested in many ways, especially for producing a small amount of potable water for small groups of people (army units, nomads,... etc.). Systems were designed and investigated at the Faculty of Petroleum and Mining Engineering at Suez-Egypt. It was operated and investigated under real environmental conditions. Theoretical study for the all experimental work was performed.

The operation of a solar distillation system coupled with a flat plate solar water heater has been investigated experimentally. Comparison of the output between coupled and stand-alone still was conducted. It was found that the productivity of the still stand alone predicated to be about $2.28 \text{ L/m}^2/10 \text{ hours}$. While the productivity of solar still coupled with flat plate solar water heater $1.56 \text{ L/m}^2/10 \text{ hours}$ in the condition with high solar intensity, so the flat plate solar water heater is effective in the condition with low solar intensity and low temperature because of the output temperature from plate solar water heater is less than the temperature of water in the basin of a passive still. In contrast, results indicate that the solar still productivity was increased and enhanced by the aid of ETC to be $6.45 \text{ L/m}^2/12 \text{ hours}$.

The comparison between theoretical and experimental investigation shows good agreement. Theoretical results were obtained from the theoretical model (Matlab program) by feed it by the weather data and conditions in January and March. The productivity vary from $1.0 \text{ L/m}^2/\text{day}$ in January to $3.0 \text{ L/m}^2/\text{day}$ in March in Suez governorate.

NOMENCLATURE

Abbreviation

A	Area (m^2)
C	Specific heat (kJ/kg K)
d	Diameter(mm)
dt	Time interval (s)
ETC	Evacuated tube solar water heater
FPC	Flat plate solar water heater
Gr	Grashoff number
h	Heat transfer coefficient; Overall heat transfer coefficient($\text{W/m}^2 \text{ K}$)
I (t)	Solar flux on an inclined collector (W/m^2)
K	Thermal conductivity($\text{W/m} \cdot ^\circ\text{C}$)
L	Latent heat of evaporation (kJ/kg)
\dot{m}	Mass flowrate(kg/s)
M	Mass (kg)
MSF	Multi stage flash desalination
Nu	Nusselt number
P	Partial pressure (N/m^2)
Pr	Prandtl number
PV	Photovoltaic
Q	Heat transfer (W)
Ra	Rayleigh number
RO	Reverse osmosis
s	Slope
t	Time(s); insulation thickness(mm)
T	Temperature($^\circ\text{C}$)

Subscripts

a	Ambient, air
av	Average
b	Basin
c	Convective
e	Evaporative; equivalent
ex	Heat exchanger
g	Glass
i	Inlet
loss	Side Loss

o	Outlet
r	Radiative
s	Surface
w	Water

Greeks

ε	Emissivity
α	Absorptivity
η	Efficiency
σ	Stefan–Boltzmann constant ($\text{W/m}^2 \text{ K}^4$)
\mathcal{B}	Coefficient of thermal expansion ($1/\text{K}$)
μ	Dynamic viscosity(N.s/m^2)
τ	Transmissivity
ρ	Density (kg/m^3)

TABLE OF CONTENTS

ACKNOWLEDGMENT	i
ABSTRACT	ii
NOMENCLATURE	iv
TABLE OF CONTENTS	vi
LIST OF FIGURES	viii
LIST OF TABLES	xi
CHAPTER 1: INTRODUCTION	
1.1. Water Shortage Problem	1
1.2. Energy Resources	4
1.3. Renewable Energy Resources	5
1.4. Solar Desalination Systems As a Choice	6
1.5. Solar Still	8
1.6. Classification of Solar Stills	9
1.7. Passive Solar Still	9
1.8. Active Solar Still	20
CHAPTER 2: LITERATURE REVIEW	
2.1. Historical Background of Desalination	21
2.5. Enhancement of Solar Still Studies	23
2.6. Research Objective	28
CHAPTER 3: THEORETICAL ANALYSIS	
3.1. Introduction	29
3.2. Proposed System	29

3.3.	Mathematical Modeling	30
3.4.	Numerical Result	36
CHAPTER 4: AN EXPERIMENTAL STUDY		
4.1.	Experimental Set Up	37
4.2.	Measurement Instrument Specification	43
CHAPTER 5: RESULTS AND DISCUSSION		
5.1.	Introduction	48
5.2.	Comparison Between Passive Solar Still and Active Solar Still	48
5.3.	Numerical result	68
5.4.	Conclusion	73
REFERENCES		75
APPENDICES		
APPENDIX A: Mathematical Model		81
APPENDIX B: Numerical and Experimental Results		87

LIST OF FIGURES

Figure	Page
1.1. Water distribution in the world	2
1.2. Nile river water	2
1.3. Types of energy	4
1.4. Flow chart of renewable energies powered desalination processes	6
1.5. World solar radiation	7
1.6. Classification of solar stills	9
1.7. A passive solar still	10
1.8. Various configurations of basin type solar stills.	10
1.9. Cascade solar still	11
1.10. Sketch of single-basin and double-basin stills	11
1.11. A schematic diagram of a multiple effect diffusion type solar still	13
1.12. Single-effect single-wick stills: (a) Wick type collector-evaporator still; (b) Modified wick-type collector-evaporator still.	14
1.13. Double-slope multi-wick solar still Top: cross sectional view	15
1.14. Titled wick solarstill	16
1.15. Hemispherical solar still	17
1.16. Concave wick solar still	18
1.17. Cooling of glass cover by (a) feedback flow, and (b) counter flow	19
1.18. Active solar still coupled with flat plate collector	20
2.1. Della Porta solar distillation apparatus	22
3.1. An active solar still coupled with evacuated tube collector	29
4.1. Experimental set-up	37
4.2. Experimental set-up schemaic diagram	38
4.3. (A) Standalone solar still, (b) solar still with heat exchanger	39
4.4. Evacuated tube collector	40
4.5. Flat plate collector	41
4.6. Recirculation pump	42
4.7. Temperature sensors (Thermocouple type K)	43

4.8.	Temperature sensors(Thermocouple type K) measure glass temperature	44
4.9.	Hanna instrument (Thermocouple type K) measure glass temperature	45
4.10.	Temperature recorder	46
4.11.	Temperature recorder	47
4.12.	Haenni solar radiation	47
4.13.	Sensor of solar radiation	47
5.1.	Hourly variation of solar intensity and ambient temperature, FPC (June 11th, 2014)	50
5.2.	Comparison between theoretical and experimental results of water temperature, FPC (June 11th, 2014)	50
5.3.	Comparison between theoretical and experimental results of glass temperature, FPC (June 11th, 2014)	51
5.4.	Experimental and theoretical accumulated productivity, FPC (June 11th, 2014)	51
5.5.	Hourly variation of solar intensity and ambient temperature, ETC (June 10th, 2014)	53
5.6.	Comparison between theoretical and experimental results of water temperature, ETC (June 10th, 2014)	54
5.7.	Comparison between theoretical and experimental results of glass temperature, ETC (June 10th, 2014)	54
5.8.	Experimental and theoretical accumulated productivity, ETC (June 10th, 2014)	55
5.9.	Hourly variation of solar intensity and ambient temperature, ETC (June 16th, 2014)	57
5.10.	Comparison between theoretical and experimental results of water temperature, ETC (June 16th, 2014)	57
5.11.	Comparison between theoretical and experimental results of glass temperature, ETC (June 16th, 2014)	58
5.12.	Experimental and theoretical accumulated productivity, ETC (June 16th, 2014)	58
5.13.	Hourly variation of solar intensity and ambient temperature, FPC (June 17th, 2014)	60
5.14.	Comparison between theoretical and experimental results of water temperature, FPC (June 17th, 2014)	61
5.15.	Comparison between theoretical and experimental results of glass temperature, FPC (June 17th, 2014)	61
5.16.	Experimental and theoretical accumulated productivity, FPC (June 17th, 2014)	62
5.17.	Hourly variation of solar intensity and ambient temperature, ETC (July 9, 2014)	63

5.18.	Comparison between theoretical and experimental results of water temperature, ETC (July 9, 2014)	64
5.19.	Comparison between theoretical and experimental results of glass temperature, ETC (July 9, 2014)	64
5.20.	Experimental and theoretical accumulated productivity, ETC (July 9, 2014)	65
5.21.	Hourly variation of solar intensity and ambient temperature, ETC (August 9, 2014)	66
5.22.	Comparison between theoretical and experimental results of water temperature, ETC (August 9, 2014)	67
5.23.	Comparison between theoretical and experimental results of glass temperature, ETC (August 9, 2014)	67
5.24.	Experimental and theoretical accumulated productivity, ETC (August 9, 2014)	68
5.25.	Hourly variation of solar intensity and ambient temperature in (January23, 201)	69
5.26.	Theoretical results of water temperature, ETC (January23, 201)	69
5.27.	Theoretical results of glass temperature, ETC (January23, 201)	70
5.28.	Theoretical accumulated productivity, ETC (January23, 201)	70
5.29.	Hourly variation of solar intensity and ambient temperature in (Mar20, 201)	71
5.30.	Theoretical results of water temperature, ETC (Mar20, 201)	71
5.31.	Theoretical results of glass temperature, ETC (Mar20, 201)	72
5.32.	Theoretical accumulated productivity, ETC (Mar20, 201)	72

LIST OF TABLES

Table	Page
1.1. Fresh water demand and desalination capacity in the Red Sea and south Sinai regions.	3
1.2. Some of indirect solar desalination pilot plants implemented at different locations	8
4.1. Hanna specification	45

CHAPTER1

INTRODUCTION

1.1. WaterShortage Problem

Water and its natural resources are considered very important part for living on the earth. Figure 1.1 shows water distribution in the world[1]. Water is very important for the proceeding of the all life needs and in all life fields like agriculture's needs, human needs and industrial needs. But at the last few decades, water shortage problems appeared at many countries especially developing countries[2]. Egypt, whose population may reach 97 million by 2025, gets essentially needs from Nile river water as shown in Figure1.2 [3]. It was anticipated that by the year 2025 water per capita will drop to about 600 m^3 that approaching the water poverty limit. The immediate action is to turn towards non-conventional sources such as waste water recycling, reuse of treated industrial and sewage effluents, rainfall harvesting and sea water desalination [4]. As an example, the geographical locations of the Red Sea natural scenarios controlled the distribution of the hotels, villages and resorts in a sporadic pattern over the long coastline, which spreads along about 1500 km. A severe shortage of fresh water in the Red Sea region and South Sinai in the year 2020 is depicted[5]. Table 1.1 shows that the great gab between the demand and the available fresh water is widening. As a result, the desalination of the Red Sea water is the only option under the expected shortage of Nile water resources.

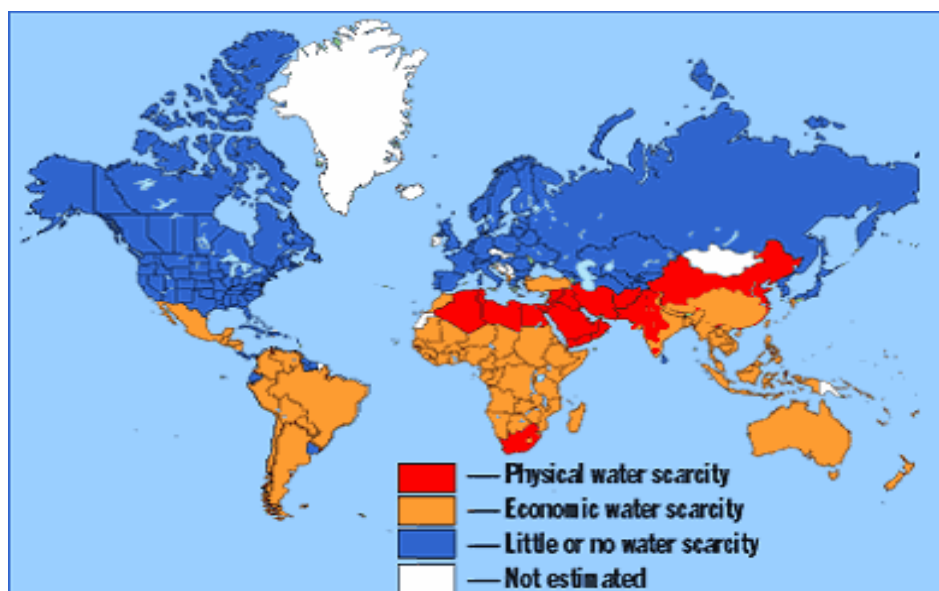


Fig.1.1: Water distribution in the world [1]



Fig.1.2: Nile river water [3]

Table 1.1: Fresh water demand and desalination capacity in the Red Sea and South Sinai regions up to 2020[5]

Year	2001		2020	
Fresh water source	Red Sea coast m³/day	South Sinai coast m³/day	Red Sea coast m³/day	South Sinai coast m³/day
Nile water pipe-line	80,000	0	140,000	30,000
Fresh ground water	0	10,000	0	25,000
Seawater desalination	97,000	40,000	250,000	150,000
Estimated demand	500,000	125,000	1,000,000	600,000
Water shortage	323,000	75,000	610,000	395,000

1.2. Energy Resources

Energy-intensive industries(e.g. oil refining, chemicals...etc.), typically use the most energy. Fossil fuels from decayed organic material through a series of chemical reactions that occur gradually over millions of years under specific physical conditions in a select group of rocks. These conditions make it possible to predict where oil and gas may be found but also highlight the fact that fossil fuels are non-renewable resources that will not be replaced once used. Reserves of oil and natural gas will probably be stretched out for another century but we must face the inevitable conclusion that these finite resources will have to be replaced with an alternative form of energy in the next 50 years [7]. The inevitable decrease in the availability of fossil fuels will be felt most acutely in transportation because there is no viable inexpensive replacement for the refined petroleum products that fuel automobiles and airplanes.

Coal represents an alternative fossil fuel with a potentially longer life span than either oil or gas but it has the unfortunate distinction of generating more pollution than the other fossil fuels. Furthermore, coal produces more carbon dioxide during combustion than either oil or gas, but all three have been fingered as the primary sources of the greenhouse gas that is the culprit for global warming. Advocates of a nuclear future have seized the potential threat of global warming and the nation's dependence on foreign oil to advance the nuclear cause.

Nuclear power predicted that electricity would be virtually free by the end of the century because of the electrical benevolence of nuclear energy. Currently only 17% of the world's electricity is generated by nuclear power and that number is unlikely to grow because of concerns about the safety of nuclear reactors and anxiety over how to dispose of highly radioactive waste produced during power generation. Rarely has a technology

shown such early promise only to fall so rapidly from grace. Figure 1.3 shows different types of energy resources.

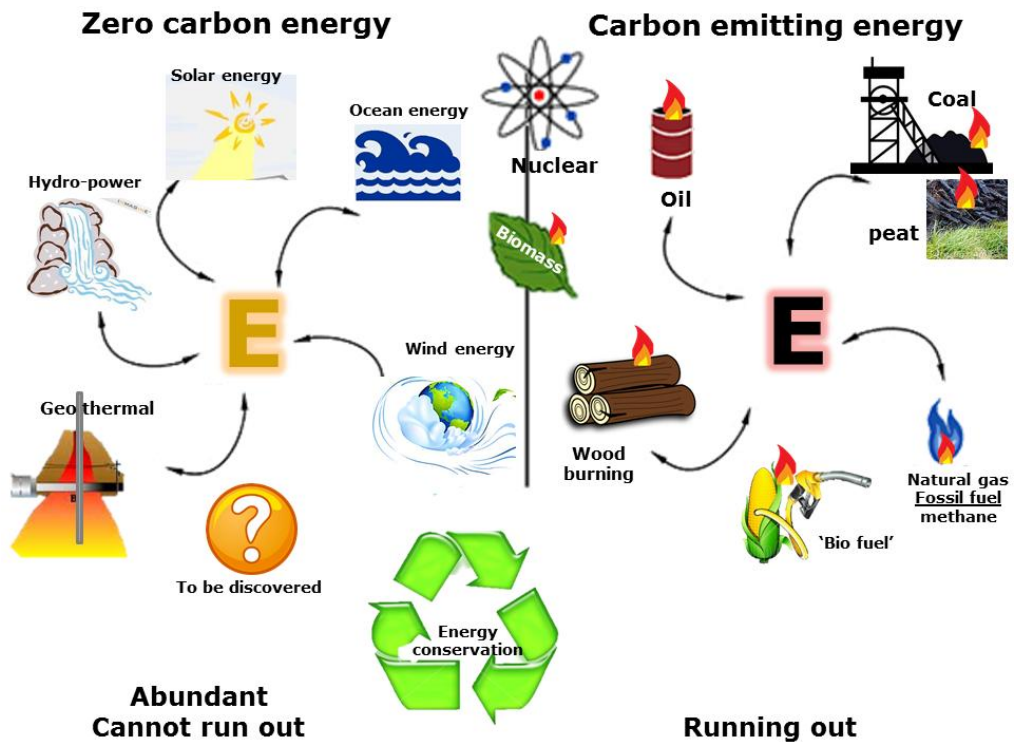


Fig.1.3: Types of energyresources [6]

1.3. Renewable Energy Resources

Current utilization of renewable energy resources (i.e. hydroelectric, wind, solar, biomass, geothermal) shown in Figure 1.3 is less than 10% of the worldwide energy generation. It has few of the drawbacks of fossil fuels or nuclear power and hold promise of a sustainable energy future. Some of these renewable energy sources have greater potential than others. Figure 1.4 shows a flow chart for renewable energy powered desalination processes [7].

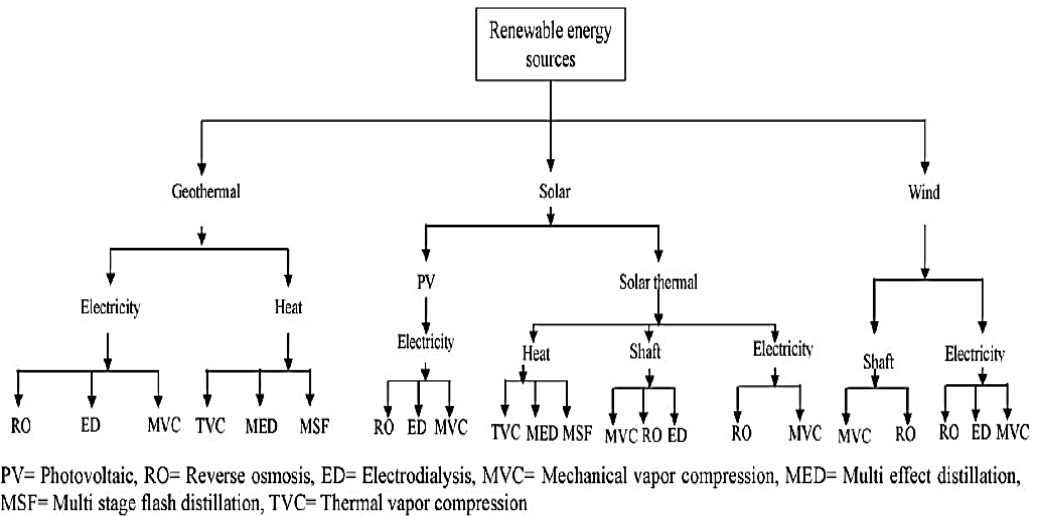


Fig.1.4: Flow chart of renewable energies powered desalination processes [8]

1.4. Solar Desalination Systems as a Choice

Desalination provides such an alternative source offering water for irrigational, industrial and municipal use. The standard techniques like multi stage flash, multi effect distillation, vapor compression and reverse osmosis are reliable for large capacity range of 100 to 50,000 m³/day of fresh water production [9]. However, these technologies are expensive for small amounts of fresh water. Moreover, they cannot be used in locations where there are limited maintenance facilities. In addition, the use of conventional energy sources to drive these technologies has a negative impact on the environment. Using solar energy is a practical method for obtaining small amounts of fresh water from saline water. Solar water distillation has been a subject of great interest for several decades. Solar desalination techniques are considered to be clean operations for producing clean water from the saline water.

Figure 1.5 shows the good presence of the solar radiation in Egypt, which is considered to be one of the high insolation countries of the world[9]. The sunshine hours are about 3600 hours/year. Also Suez-Gulf region is considered to be one of the highest insolation regions in Egypt. The average daily insolation that hits this region is found to be varying from 3.5 to 7.2 kWh/m²/day throughout the year. That for some geographical reasons like nearest from the sea level, the seasonal rainfall hours almost low and the weather is always hot and dry. So, it is very important to utilize this present huge energy in Egypt (Suez-Gulf) in desalination technologies (small and large sizes).

Techniques of solar desalination are many and varying according to the size of the demanding of fresh water and the size of solar energy presence. Table 1.2 illustrates some of desalination processes powered by solar energy [9].

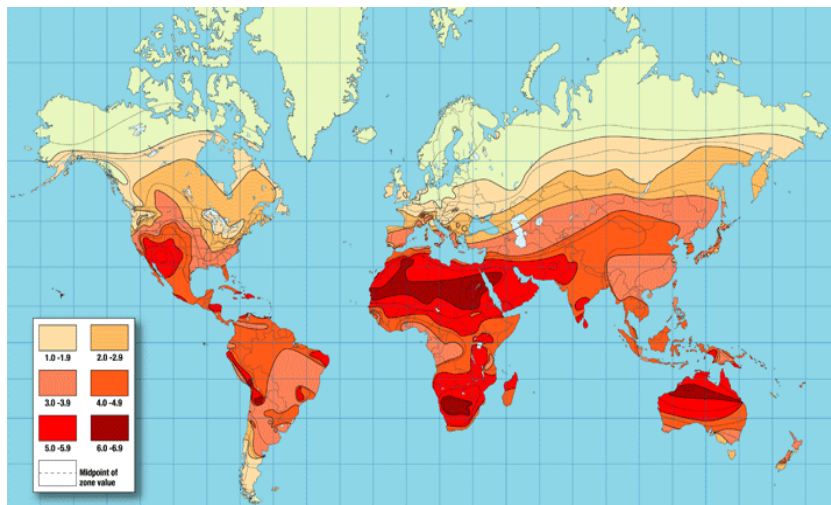


Fig.1.5: World solar radiation[10]

Table 1.2: Some of indirect solar desalination pilot plants implemented at Different location

Desalination process type	Location	Capacity	Type of power	Reference
MSF	Safat, Kuwait	10m ³ /day	Solar collectors	[11]
MSF	Al Azhar University in Gaza	0.2m ³ /day	Solar thermal collectors and PV cells	[12]
MSF	Berken, Germany	10m ³ /day	--	[13]
MSF	Gran Canaria, Spain	10m ³ /day	Low concentration solar collectors	[14]
MSF	Lampedusa Island, Italy	0.3m ³ /day	Low concentration solar collectors	[15]
MSF	La Paz, Mexico	10m ³ /day	Flat plate and Parabolic trough collectors	[16]
MSF	Kuwait	100m ³ /day	Parabolic trough collectors	[17]
MSF+MED	Al-Ain, UAE	500m ³ /day	Parabolic trough collectors	[18]
PV+RO		1m ³ /day	PV	[19]

1.5. Solar Still

Solar stills can provide a solution for those areas where solar energy is available in plenty but water quality is not suitable for human use. Solar still device can be used for producing drinking water. These devices are cheap and having low maintenance cost but its low productivity [20&21]. Solar stills can be used for low capacity and self-reliance water supplying systems since they can produce drinking water by solar energy only, and do not need other energy sources such as fuel or electricity.

1.6. Classification of Solar Stills

The methods of solar water desalination can be classified according to the way in which the solar energy used, as shown in Figure 1.6.

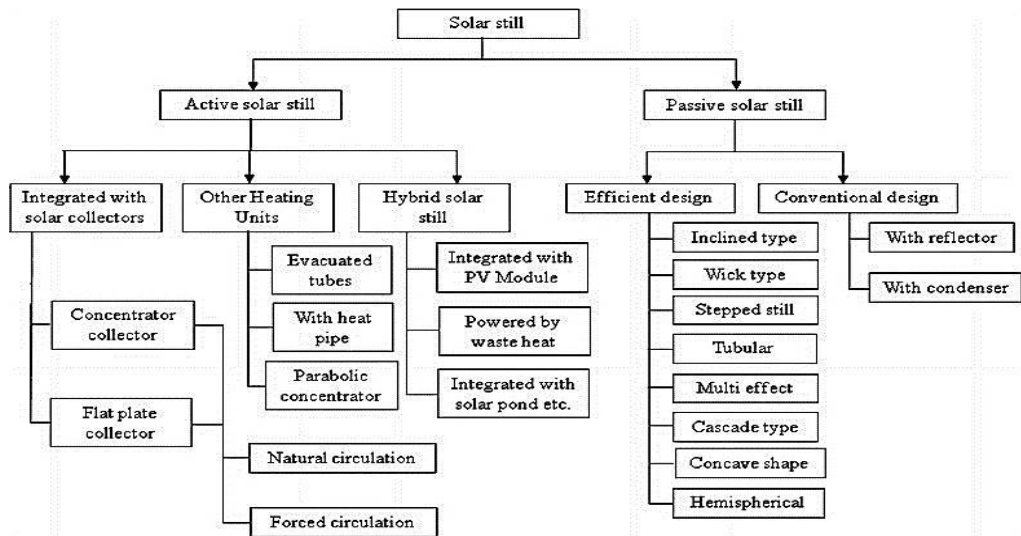


Fig.1.6: Classification of solar stills[22]

1.7. Passive Solar Still

Passive solar stills illustrated in Figures 1.7 to 1.9 have been manufactured all over the world. The following are the main types of passive basin type solar stills:

- Single slope solar still
- Symmetrical doubled-sloped type with continuous basin
- Symmetrical doubled-sloped type with separate bays
- Unsymmetrical doubled sloped type
- Inverted vee type
- Cascade solar still type, Figure 1.9

Generally for solar still shown in Figure 1.8 [23], types (a), (b), and (c) use glass covers, while type (d) uses plastic covers.

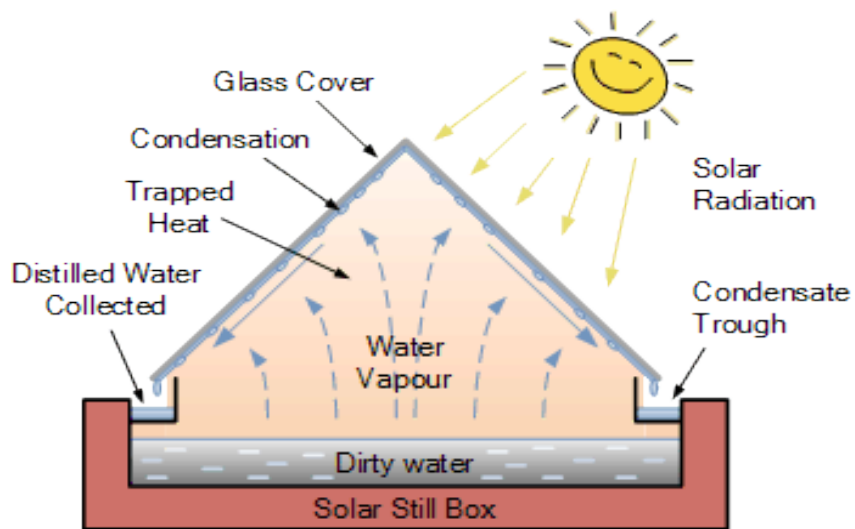


Fig.1.7: Passive solar still [24]

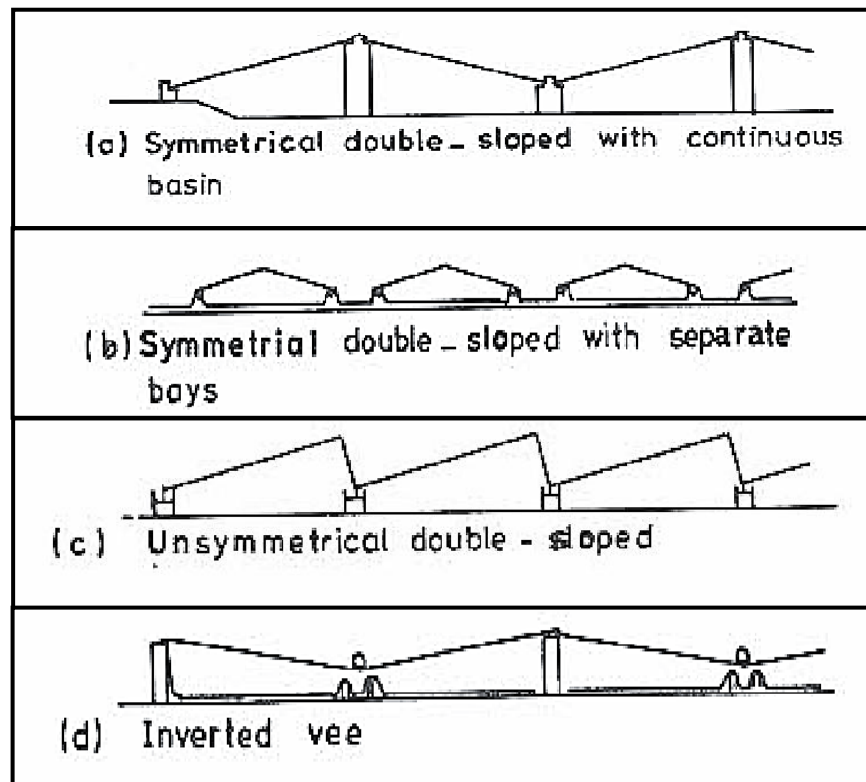


Fig.1.8: Various configurations of basin type solar stills [25]

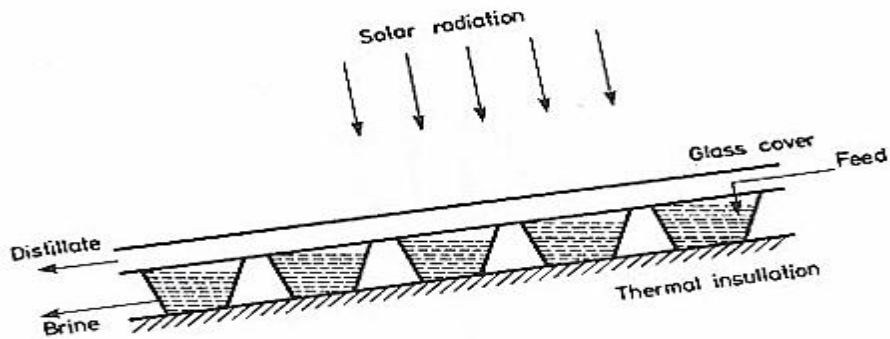


Fig.1.9: Cascade solar still, [26]

1.7.1 Classification of basin solar stills

- **Single-slope versus double-slope basin stills**

Comparison of the two configurations of basin type stills shown in Figure 1.10, single slope and double slope basin stills, the maximum radiation may be higher in double-slope stills. A single slope still gives better performance than a double slope for cold climatic conditions. For summer climatic conditions the double slope gives better performance. The first basin glass cover is used as the base for the second basin with the advantage that the heat of condensation from the first basin cover is used to heat the water on the bottom of the second basin [27].

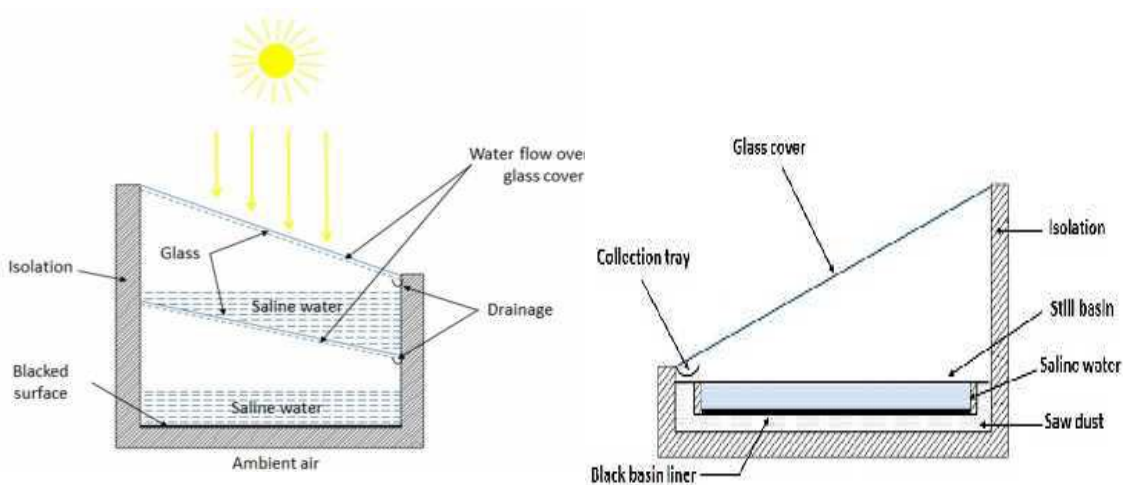


Fig.1.10: Sketch of single-basin and double-basin stills [28]

1.7.2 Diffusion stills

1.7.2.1 Basic diffusion still

Fatah and El Sherbiny [29] showed that daily yield of diffusion still varies between 0.5 and 5.0 kg/m² under climatic conditions of Egypt. Based on a similar design, operational and environmental parameters, El-sayed [30] numerically compared single-effect diffusion still with a basin-type still. The theoretical results showed that the use of the diffusion-type still leads to an improvement in both production rate and operational efficiency.

1.7.2.2 Multiple effect diffusion

Multiple effect diffusion type solar still has great potential because of high productivity and simplicity. Multiple effect diffusion type solar still shown in Figures 1.11 consists of a flat plate reflector, casters for manual azimuth tracking and vertical multiple effect diffusion type still, which consists of a glass cover and number of vertical and parallel partitions with narrow gaps between partitions. The height of the still is 1 m. Length of the flat plate reflector is 1 m. Width of the still and flat plate reflector is 1 m. A diffusion gap between partitions is 5 mm. Air gap between the glass cover and first partitions is 10 mm. Absorptivity of the front surface of the first partition for sun ray is 0.9. Emissivity of glass cover is 0.9, and total number of partitions is 10. The saline water is fed to the wicks constantly. The angle of the flat plate reflector and azimuth angle of the still can be adjusted manually to absorb solar radiation on first partition effectively according to locations and seasons. Both direct and diffuse solar radiation, and the solar radiation reflected by the flat plate reflector transmit through the glass cover and are absorbed on the front surface of the partition to cause the evaporation of saline water[31].

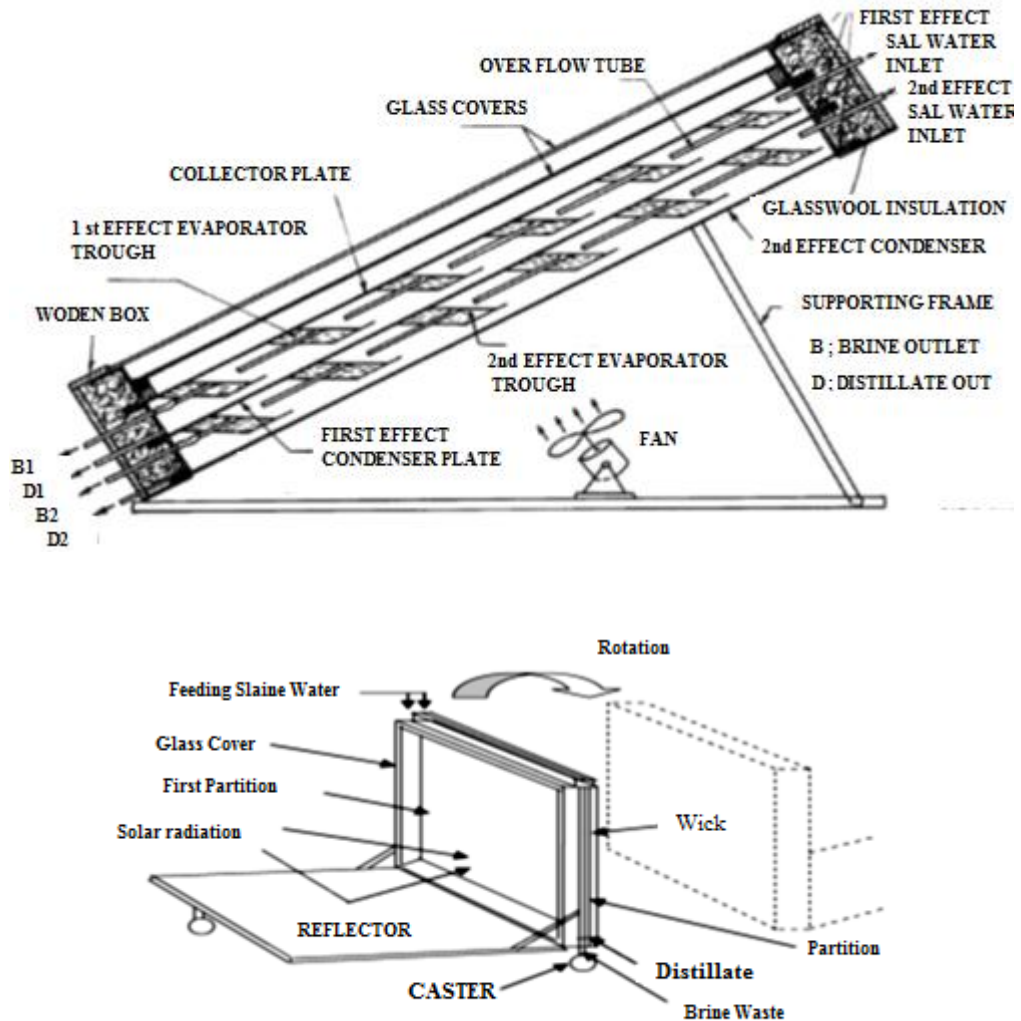


Fig.1.11: Schematic diagram of a multiple effect diffusion type solar still [32]

1.7.3 Wick solar still

1.7.3.1 Single-wick still

The results of a still of this type using a plastic cover located at Valparaiso, Chile, showed a production rate of 3.8 to 4.4 l/m²/day with an operational efficiency about 40-46% [33]. An improved design for the wick-type collector evaporator still in Figure 1.12 had been investigated

by Moustafa et al [34]. The results of this design showed a production rate of 4.4 to 6.12 l/m²/day with an operational efficiency about 58%.

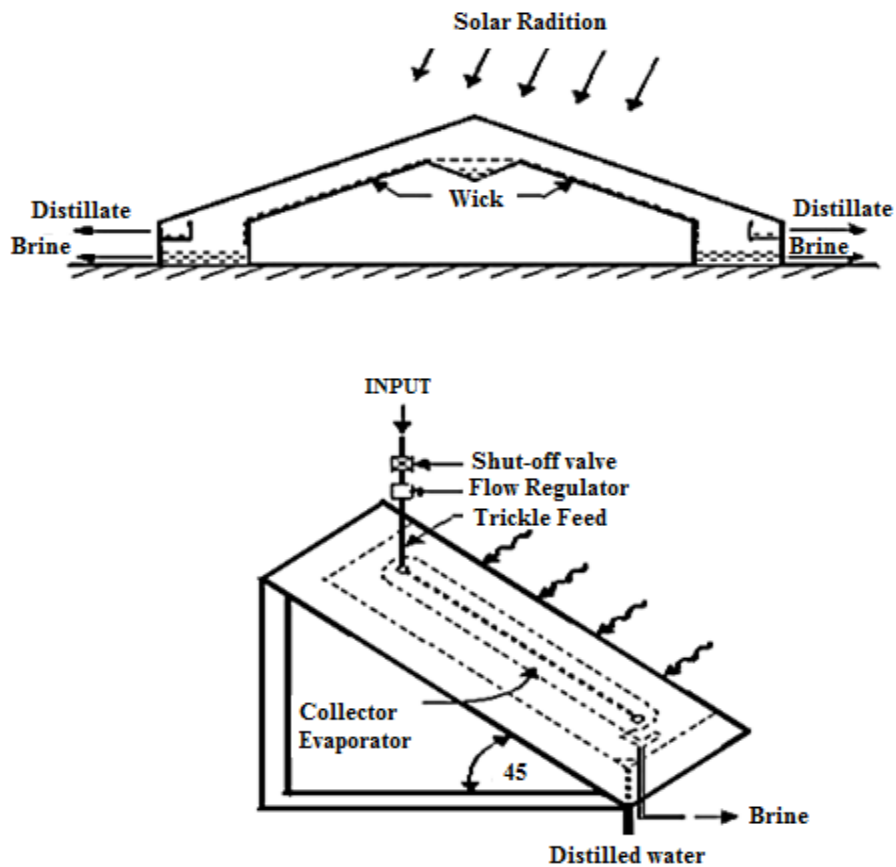


Fig.1.12: Single-effect single-wick stills: (a) Wick type collector-evaporator still; (b) Modified wick-type collector-evaporator still [35]

1.7.3.2 Multi-wick stills:

Tiwari et al [36] Proposed double-condensing, multi-wick still. Excess vapor can then be condensed on the additional surface and reduce the heat load on the glass cover, reduces glass cover temperature, which in turn enhances evaporation rate. The experimental results showed a 20% increase in the still productivity over the simple multi-wick still. Figure 1.13 shows a cross-sectional view and plant layout of a double-slope multi-wick solar distillation unit that was installed in Delhi, in 1981.

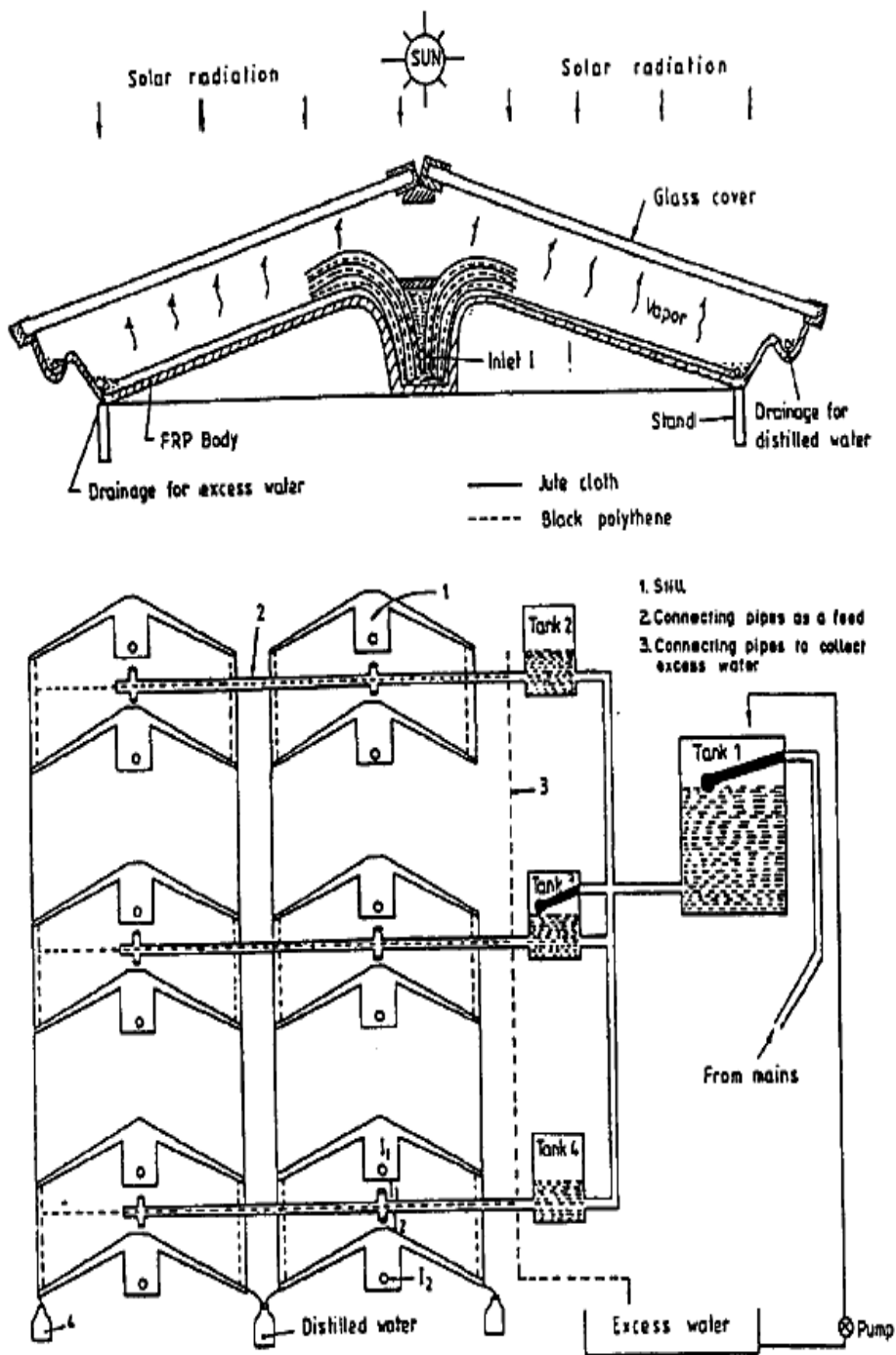


Fig.1.13: Double-slope multi-wick solar still. Top: cross sectional view, Bottom: distillation plant layout [36]

1.7.3.3 Tilted wick solar still

It has already been established that a reduction in the depth of brine in the still improves the productivity, mainly due to the higher basin temperature. The advantage of the wick still shown in Figure 1.14 is to keep the brine as shallow as possible (with low heat capacity) while avoiding dry spots.

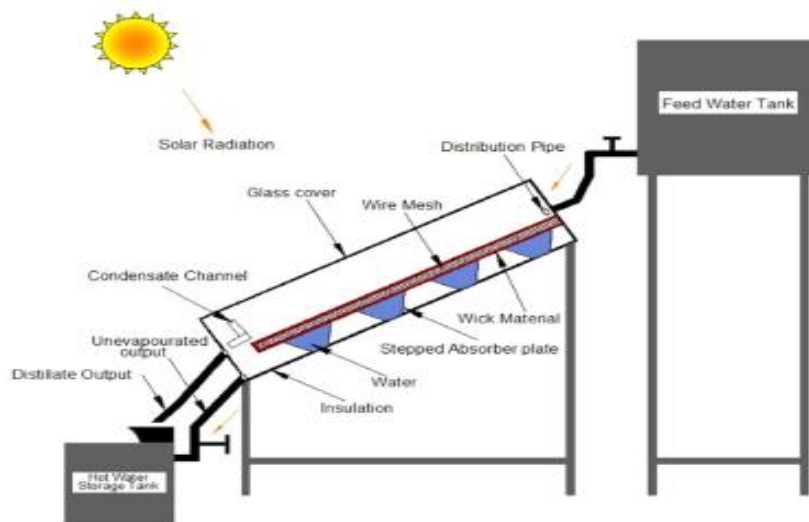


Fig. 1.14: Titled wick solar still [37]

1.7.3.4 Wick versus basin stills:

The productivity of the multi-wick stills is always higher than conventional basin stills due to the negligible heat capacity of the water mass in the multi-wick stills. Tiwari et al. [38] indicated that the multi-wick distillation plant will be more economical for a medium-scale installation. For larger scale supply of distilled water, the basin type is preferred because of its simplicity and low cost.

1.7.3.5 Combined wick-basin stills:

Connection of a conventional basin type still (installed in a shadow and having an opaque cover) with a wick-type solar still and hot waste brine water leaving the wick-type feeds directly into the basin-type with cooled cover of basin still. The combined stills showed higher efficiency than the two stills separately, and the yearly amount of distilled water was 85% more than the basin type and 43% more than the wick type [39].

1.7.4 Other types of solar stills

1.7.4.1 Hemispherical solar still

T. Arunkumar [40] proposed a new design of solar still with a hemispherical top cover for water desalination with and without flowing water over the cover as shown Figures 1.15. The daily distillate output of the system is increased by lowering the temperature of the cover by water flowing over it. The recorded efficiency was 34%, and it was increased to 42% with the top cover cooling effect. Variations of a few important parameters were measured during field experiments such as water temperature, cover temperature, air temperature, ambient temperature and distillate output, and solar radiation incident on a solar still.

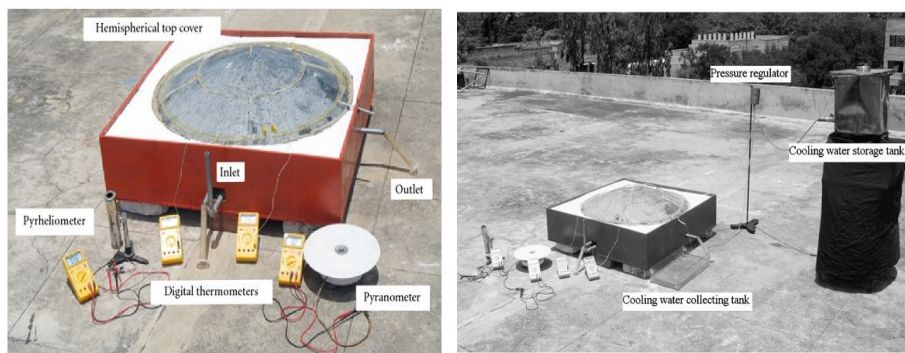


Fig.1.15:Hemispherical solar still [40]

1.7.4.2 Concave surface Solar still

A concave shaped wick surface increases an evaporation rate because the water surface level is lower than the upper limit of the wick surface as indicated in Figure 1.16. Results show that average distillate productivity in day time was 4.1 L/m² and the maximum instantaneous system efficiency was found to be 45% and the daily efficiency of the still was 30%. The maximum hourly yield was 0.5 L/h per m² after solar noon [41].

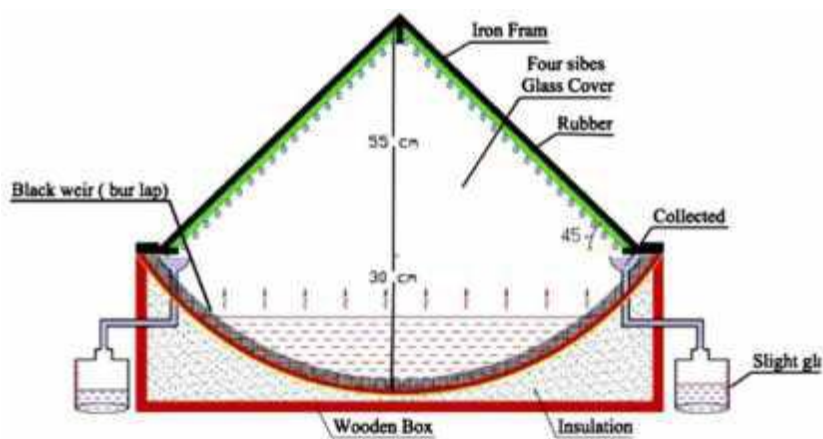


Fig. 1.16: Concave wick solar still [41]

1.7.4.3 Still with cover cooling

Evaporation rate can be increased if the difference in temperature between the basin (heat sources) and the glass cover (heat sink) increases. This can be achieved by either increasing the basin temperature or decreasing the cover temperature or both. Two cooling arrangements have been suggested, both using a double glass cover. These two methods are shown in Figure 1.17, and are termed feedback flow and counter flow. Results have shown that cover cooling produces an increase in the productivity of the still, with the improvement when using the feedback flow being greater than when using the counter flow[30]. Since part of the sensible heat gained by cooling the glass cover is utilized in the feed.

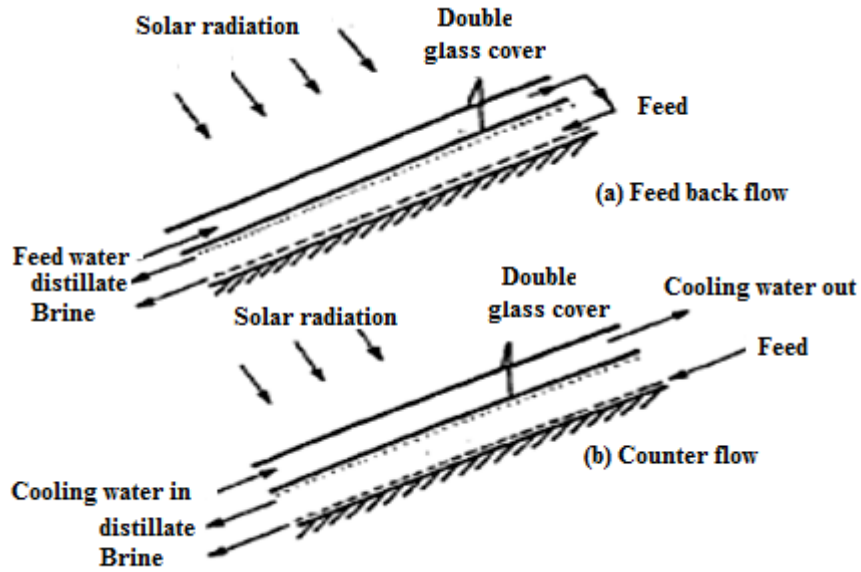


Fig.1.17: Cooling of glass covers by (a) feedback flow, and(b) counter flow, [30]

1.7.4.4 Black dye/muddy water still

Lawrence et al. [42] indicated that: (a) there is a significant effect of dye on still performance particularly for large water depth, and (b) black dye gives a better performance than violet and red dyes.

Muddy water is opaque, and so the incident solar radiation gets absorbed mostly around the top layer. The results for distillation of muddy pond water indicated (on the daily basics) that the muddy and clear water samples yielded the same distillate output[38]. Not much information is available on muddy and polluted water, which in some regions of the world may be the only source of feed water.

1.8. Active Solar Still

There is a lot of researchers used many techniques to produce a new systems combined between the solar water heater and solar still as shown in Figure 1.18 to improve the productivity and performance. Brackish water is circulated to solar collector to be preheated before entering solar still. Due to sun radiation, water gets evaporated and collected on glass cover from where it flows towards distillate channel. It is concluded that passive solar stills can be economical to provide potable or distilled water. On the other hand, active solar still can be economical from a commercial point of view.

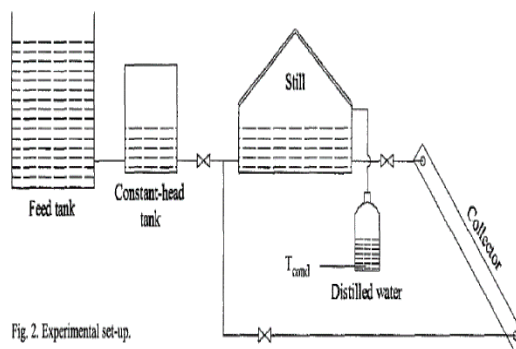


Fig.1.18: Active solar still coupled with flat plate collector, [43]

CHAPTER 2

LITERATURE REVIEW

2.1. Historical Background of Desalination

A historical review may help to understand the main concept of desalination processes through last centuries. Delyannis [44] has studied the point of what history of desalination processes mean. In his research he tried to overpass historical paths by focusing on the most important ideas and features developed from antiquity until today on desalination of non-potable with special reference to the use of solar energy for desalination. He found that the sun was especially glorified by the Egyptians, Greeks, and Incas. Looking at the mankind history, can find that energy and water are correlative items that govern civilization life.

The desalination concept from pre-historic times to middle ages

Of all philosophers of antiquity it is the well-known scientist, Aristotle (384–322), who described in a surprisingly correct way the origin and properties of natural, brackish and seawater. He writes for the water cycle in nature:

The sun moving, as it does, sets up processes of becoming and decay, and sweetest water is every day carried out and is dissolved into vapor and rises to the upper regions, where it is condensed again by the cold and so returns to the earth. Even today no better explanation is given for the water cycle in nature. Really, the water cycle is a huge solar 21 energy open distillation plant. Mouchot (1869, 1879) the well-known French scientist who experimented with solar energy, mentions in one of his numerous books that during medieval times Arab alchemists carried out experiments with polished Damascus concave mirrors to focus solar radiation onto glass vessels containing salt water in order to produce fresh water.

The development of solar desalination during the Renaissance period

Later on during the Renaissance, Giovanni Batista Della Porta (1535–1615), one of the most important scientists of his time wrote many books. In the volume on distillation he mentions seven methods of desalination, but the most important reference is in the 19th volume, [44] where he describes a solar distillation apparatus that converted brackish water into fresh water (Della Porta).

In 1870 the first American patent on solar distillation was granted to Wheeler and Evans the inventors described the greenhouse effect, analyzed in detail the cover condensation and re-evaporation, discussed the dark surface absorption and the possibility of corrosion problems. High operating temperatures were claimed as well as means of rotating the still in order to follow the solar incident radiation. Two years later, in 1872, an engineer from Sweden, Carlos Wilson, designed and built the first large solar distillation plant, in Las Salinas, Chile (Harding, 1883).

2.2. Enhancement of Solar Still Studies

Khalifa and Hamood. [45] conducted an experimental investigation for the effect of the insulation thickness on the solar still productivity. All sides of the basin should be well insulated to maximize the efficiency of the still. A comparison was made between a study of solar stills with insulation thickness of 30, 60 and 100mm and with those without insulation. It was found that there is a dramatic difference in productivity. The insulation thickness could influence the productivity of the still by over 80%. A number of research works were carried out and nearly all studies reported improvement in the productivity of stills due to the use of insulation. The maximum thickness of insulation that was examined in these studies 100 mm, which indicates a general, agreement between the investigators about the maximum practical thickness; they however, disagree about the limit

of the optimum thickness. This limit is ranging from 40 to 100 mm of insulation thickness. It was found that good insulation of solar stills increases the maximum brine temperature by 67%. The experimental results show that insulation could influence the productivity of the still by over 80%. The experimental data shows the productivity as a function of the insulation thickness as follow:

$$y = 1023(t) - 408.8(t) + 45.34(t) + 1.81, R = 1$$

Where

(y) is the productivity (l/m^2 day) and (t) is the insulation thickness (m),
(Root Mean square value R^2)

Nafey et al. [46] investigated the productivity enhancement of solar still in either sides theoretically and experimentally by adding floating perforated black plate to the brackish water in different brine depths (3, 4, 5, 6mm) under the same conditions. The theoretical and experimental results showed that at a brine depth of 3 cm, the increase in productivity amounted to 15% and to 40% at 6 cm of brine depth. The higher percentage in productivity is obtained in the higher brine depth because the floating plate has the advantage of maintaining the thermal energy in the water below it in a small quantity with respect to that in the plain water still. It can be said that using a floating perforated black plate in a solar still at a brine depth of 6 cm enhances the productivity by nearly 40% approximately.

Hiroshi Tanaka [47] presents theoretical analysis for a basin type solar still with internal and external reflectors. The external reflector is a flat plate that extends from the back wall of the still, and can be manually inclined forwards or backwards according to the month. A report of a theoretical prediction of the daily amount of distillate produced by the still

throughout the year was combined with this study according to previous studies, which varies according to the inclination angle of both the glass cover and the external reflector, at 30°N latitude.

Akash et al. [48] studied the effect of absorbing materials on the performance of a double slope single basin solar still. The results indicate that the productivity increased by 38% by adding absorbing black rubber mat to the basin. Using black ink, the productivity was increased by 45% and by using black dye (being best absorbing material) the water productivity enhancement by 60%.

Arjunan et al. [49] carried out experimental study in a try to store the excess solar radiation energy by putting blue stones in the still basin. It was observed that the productivity of the still is influenced by the internal and external heat transfer with keeping the glass cover at 10° tilt angle, paralleled with a conventional still and there is 5 % increase in the productivity of the modified solar still when using blue metal stones as a storage medium. They observed that the maximum amount of heat loss takes place in the solar still is a mixed effect of convective and radiation heat transfer from glass to ambient.

Tiwari and Tiwari [50] conducted an experimental study for five days for different five water depths from 0.04m to 0.18m. They observed the effect of water depth on evaporative mass transfer coefficient. They concluded that heat transfer coefficient depends significantly on water depth.

Mahmoud. et al [51] investigated the performance of a multi-stage water desalination still connected to a heat pipe evacuated tube solar collector with aperture area of 1.7 m². The multi-stage solar still water desalination system was designed to recover latent heat from evaporation and condensation processes in four stages. The variation in the solar radiation

during a typical midsummer day in the Middle East region was simulated on the test rig using an array of 110 halogen floodlights covering the area of the collector. The experimental results demonstrated that the system produces about 9 kg of fresh water per day and has a solar collector efficiency of about 68%. However, the overall efficiency of the laboratory test rig at this stage of the investigations was found to be at the level of 33% due to excessive heat losses in the system. The analysis of the distilled water showed that its quality was within the World Health Organization guidelines. The still's operation was numerically simulated by employing a mathematical model based on a system of ordinary energy and mass conservation differential equations written for each stage of the still. A computer program was developed for transient simulations of the evaporation and condensation processes inside the multi-stage still. Experimental results and theoretical predictions were found to be in good agreement.

Sodha et al. [52] presented the results of experimental study of waste hot water for desalination. The study was on two modes: (i) Feeding waste hot water obtained from thermal power plants once a day, (ii) Flowing waste hot water from thermal power plants at constant rate through a solar still. It was clear that the depth of water in basin, solar radiation, length of the still and inlet water temperature are the parameters which affect the performance of the still. The still fed with hot water at constant rates gives higher yield in comparison to a still with hot water filled only once in a day.

Gnaneshwar and Nimplakhandan [53] designed a solar still which maintained a vacuum in the evaporating chamber, exploiting the natural gravity law and the barometric pressure head and developed a model. They demonstrated a correlation between the predictions made by the

theoretical model with the measured performance data and produced a yield of $7.5 \text{ L/m}^2\cdot\text{day}$. With the addition of (PV/T) panel of 6 m^2 area the system produced $12 \text{ L/m}^2\cdot\text{day}$ of fresh water.

Al-Kharabsheh, Yogi Goswami [54] studied utilizing vacuum conditions for evaporation and condensation. The proposed a desalination system consisted of a solar heating system, and an evaporation chamber and a condenser. The condenser is placed 10 m above the ground level and connected to saline water via connected pipes. By balancing the atmospheric and the hydrostatic pressures in the supply and discharge pipes. The distillation of water at a lower temperature level requires less thermal energy. This heat can be provided from solar collectors, which will operate at a higher efficiency because of lower collector operating temperatures. Simple flat plate collectors may be used to heat the saline water in the evaporator. As a result of evaporating the saline water, the salinity increase which causes decreasing in evaporation rate, that is why it is necessary to withdraw the brine at a certain flow rate. As saline water in the evaporator starts evaporating, its salinity increases which tends to decrease evaporation rate, so it becomes necessary to withdraw the concentrated brine at a certain flow rate and inject saline water at a rate equivalent to the withdrawal plus evaporation rates. The withdrawn water will be at a temperature equal to that of the evaporator, so it becomes necessary to recover the energy from it. A tube in-tube heat exchanger is used for this purpose, where injected water flows inside the inner tube and withdrawn water will flow in the annulus in a countercurrent direction. Water can be injected by the atmospheric pressure under the influence of vacuum conditions. This makes the proposed system a continuous process type. It was found that the effects of withdrawal rate and the depth of water in the evaporator were small while the effect of heat source temperature was signifi-

cant. Based on theoretical simulations, the present system would perform much better than a simple flat basin solar still.

Tiwari et al. [55] developed thermal models for all types of solar collector integrated active solar stills based on energy balance equations in terms of inner and outer glass temperature. The authors have drawn the following points: (i) The overall average thermal and exergy efficiency of FPC integrated active solar still are in the range of 5.6–19.1 and 0.25–0.85%, respectively. (ii) The overall thermal efficiency of active solar stills integrated with FPC, concentrating collector, ETC and ETC with heat pipe is 13.14, 17.57, 17.22 and 18.26%, respectively. (iii) The maximum values of total heat transfer Coefficient (h) for active solar stills integrated with flat plate collector, concentrating collector, evacuated tube collector and ETC with heat pipe are 43, 86, 67 and 76 W m⁻²C⁻¹, respectively. If the exergy out from FPC is considered, then average exergy efficiency of active solar still varies in the range 0.59–1.82%.

Mohamad et al [56] conducted experimental investigate for three unsymmetrical solar stills with different insulation under actual field conditions. Also, a simple economic evaluation of solar distillation was made to find out the best insulating material, to be used in the asymmetrical solar stills. From the experimental results, an empirical correlation for the daily production from the stills is deduced. The results also show that the daily production of the stills increases by about 35% as the mean ambient air temperature increases from 17 to 30°C at the same daily total solar radiation and the same thermal insulation. From an economic point of view, it is found that dry sawdust is the best material to be used for insulating the asymmetrical solar stills.

2.3. Research Objective

It is obvious from literature review that solar still productivity can be enhanced when coupled with a solar water heater.

The main objectives of the present work can be summarized as follows:

- 1- Investigating thermal performance of passive solar still and similar solar still coupled with solar water heaters under actual condition of Suez, Egypt.
- 2- Developing a simulation program to predict the productivity of the units under investigation.

CHAPTER (3)

THEORETICAL ANALYSIS

3.1. Introduction

Theoretical study is made to develop a mathematical model in order to be able to predict thermal performance of a solar still coupled with solar water heater.

3.2. Proposed System

A schematic diagram for the proposed system is shown in Figure 3.1 the system consists of solar still connected with solar water heater and circulation pump to circulate the hot water between solar still and solar water heater via a heat exchanger.

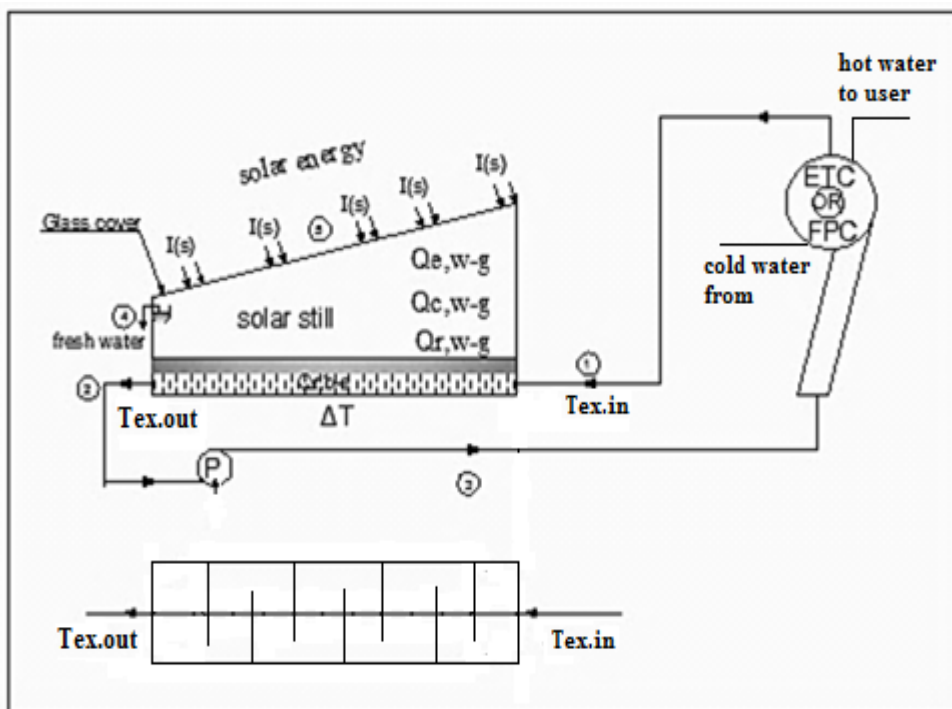


Fig.3.1:Active solar still coupled with a solar collector.

3.3. Mathematical Modeling

Using the measured values of solar intensity, ambient temperature at Suez area as input data, the daily productivity of the solar still can be calculated. The mathematical model is developed according to the relations of heat transfer coefficients, which were obtained by Gwaande [57]. The energy balance equations of the solar still could be written and presented based on the following assumptions:

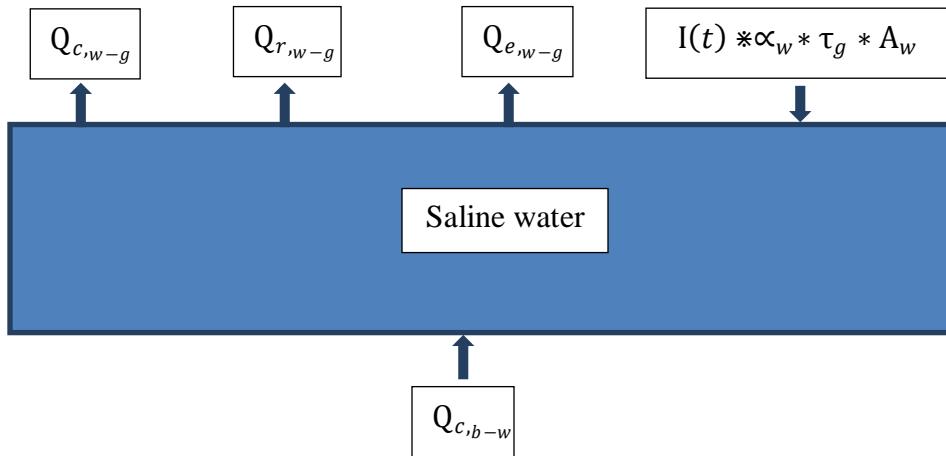
1. The glass cover has the same area A_g as the water film A_w .
2. The water film and the glass cover are gray surfaces.
3. The water film is maintained at a constant temperature T_w .
4. The glass cover is taken at a constant temperature T_g .
5. Temperature gradient across the thickness of the glass cover is neglected.
6. Heat transfer coefficient is considered to be constant at the selected time interval.
7. Heat capacity of the basin liner and the insulation is neglected.
8. The saline water in the basin is treated as fresh water.
9. The variations in the absorptivity and transmissivity of the glass and water surfaces with the variation in angle of the incoming radiation are neglected
10. There is constant and equal specific heat C_p for feed water and distillate.
11. The glass cover is exposed only to the sky.
12. Change in heat capacity of solar still element is neglected.

3.3.1 Heat analysis in a passive solar still

Energy received by the saline water in the still (from sun and base) is equal to the summation of energy lost by convective heat transfer between water and glass, radiative heat transfer between water and glass, evaporative heat transfer between water and glass and energy gained by the saline water.

- The energy balance for the saline water can be represented as follows:

$$Q_{c,b-w} + I(t) * \alpha_w * \tau_g * A_w = Q_{c,w-g} + Q_{e,w-g} + Q_{r,w-g} \quad W \quad (1)$$

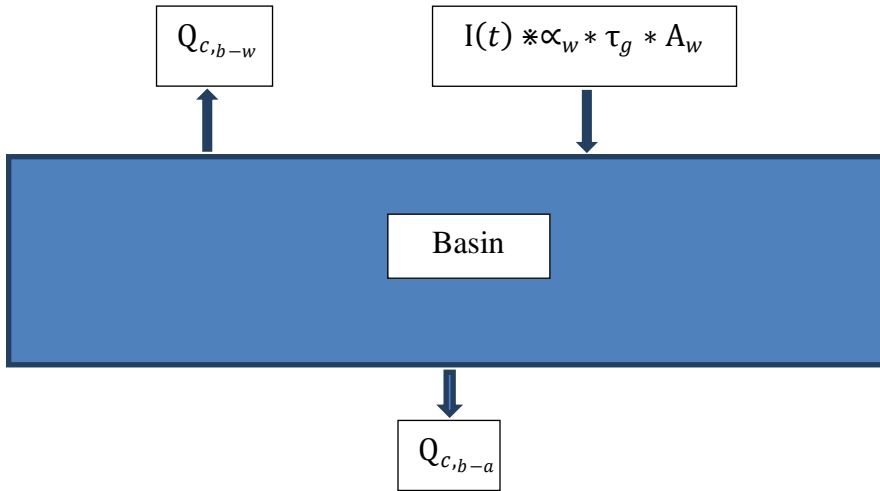


- The energy balance equation for the basin

$$Q_{c,b-w} = (A_b * I_b * \alpha_w * \tau_g) - Q_{c,b-a} \quad W \quad (2)$$

$$Q_{c,b-a} = h_b A_b (T_b - T_a) = Q_{losses} \quad W \quad (3)$$

$$Q_{c,b-w} = I(t) * \alpha_b * \tau_g * A_b - h_b A_b (T_b - T_a) \quad W \quad (4)$$



- **The energy balance equation for the glass cover**

Reference to Mostafa et al.[58] the energy balance for glass cover can be represented as follows:

$$Q_{r,g-sky} + Q_{c,g-a} = Q_{c,w-g} + Q_{e,w-g} + Q_{r,w-g} + (I(t) * \alpha_g * \tau_g * A_g)W \quad (5)$$

$$Q_{r,g-sky} = A_g * (\epsilon * \sigma * ((T_g + 273)^4 - (T_{sky} + 273)^4))W \quad (6)$$

$$T_{sky} = T_a - 10 \quad ^\circ C \quad (7)$$

$$\epsilon = (1 / ((1/\epsilon) + ((1 - \epsilon_g) / \epsilon_g))) \quad (8)$$

$$\epsilon = (1/2 * (1 + \cos(s))) \quad (9)$$

$$Q_{c,g-a} = (h_{c,g-a} * A_g * (T_g - T_a))W \quad (10)$$

$$h_{c,g-a} = a + b(V_a)^n \quad W/m^2.K \quad (11)$$

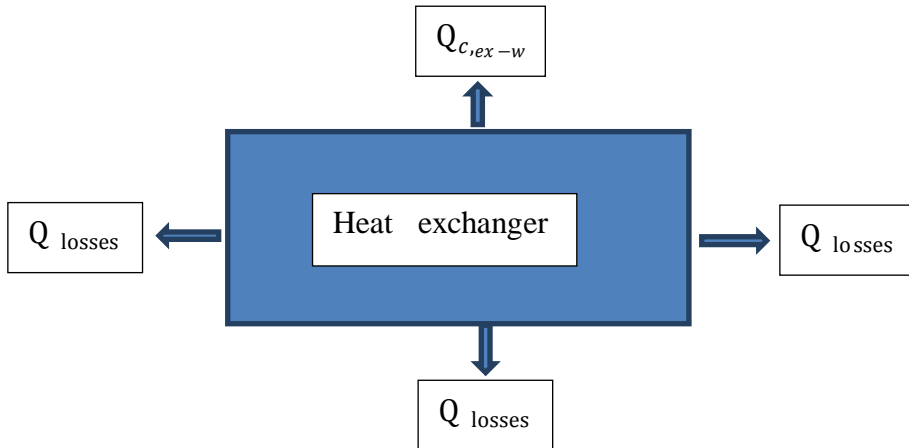
3.3.2 Heat analysis in active solar still

- Heat analysis in heat exchanger

$$Q_{C,ex-b} = M_{ex} c_p \Delta T - Q_{losses} \quad \text{W(12)}$$

$$Q_{losses} = h_{eq} A_{ex} (T_{ex} - T_a) \quad \text{W (13)}$$

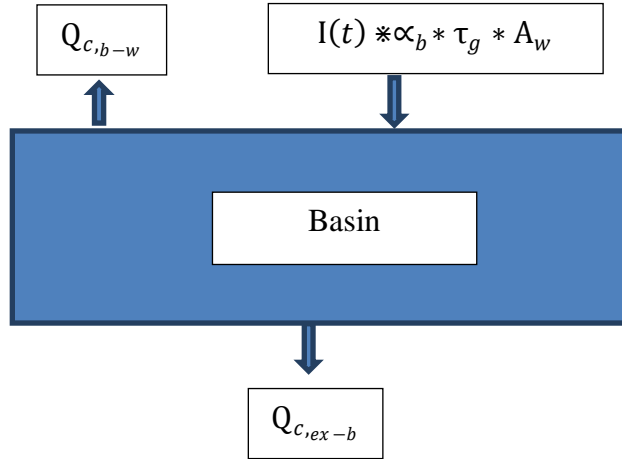
$$T_{ex} = T_{av} = (T_{out} + T_{in})/2 \quad \text{°C(14)}$$



- Heat analysis in basin

$$Q_{c,b-w} = Q_{C,ex-b} - Q_{c,b-a} + I(t) * \alpha_b * \tau_g * A_b \quad \text{W} \quad (15)$$

$$Q_{c,b-w} = I(t) * \tau_g * \alpha_b * A_b + Q_{C,ex-b} \quad \text{W} \quad (16)$$



The internal heat transfer coefficient; heat transfer from water to glass cover inside the solar still is done by three possible ways called evaporation, convection and radiation, Hence Total internal heat transfer coefficient of solar still is sum of all three possible ways heat transfer coefficients,

$$h_1 = h_{c,w-g} + h_{r,w-g} + h_{e,w-g} \text{ W/m}^2.\text{K} \quad (18)$$

Where,

h_1 is total heat transfer coefficient and $h_{c,w-g}$, $h_{r,w-g}$, $h_{e,w-g}$ are called convective, evaporative and radiative heat transfer coefficients.

3.3.3 Overall thermal efficiency of solar still

Efficiency of solar still is simply defined as the ratio between thermal energy utilized to get distillate water in certain time and energy supplied to solar still during the same time.

- **Passive solar still**

The overall thermal efficiency of passive solar still is given by:

$$\eta = \frac{\sum_{i=1}^{24} \dot{m}_{ew} L}{I(t) A_b} \times 100 \quad (19)$$

- **Active solar still**

The overall thermal efficiency of active solar still is given by:

$$\eta_{active} = \frac{(\sum_{i=1}^{24} \dot{m}_{ew} L) + (\sum_{i=1}^{24} \dot{m}_{hw} c_p (T_{wo} - T_{wi}))}{\sum_{i=1}^{24} I * (A_b + A_c)} \quad (20)$$

3.3.4 Productivity of solar still

- **Hourly yield**

The hourly yield is given by the following equation:

$$\dot{m}_{ew} = \frac{Q_{e,w-g}}{L * A_b} \text{ kg/m}^2 \cdot \text{hr} \quad (21)$$

Where

\dot{m}_{ew} ... is the distillate yield obtained in $\text{kg/m}^2 \cdot \text{hr}$ and

- **Daily yield**

The total daily yield is given by:

$$M_{ew} = \sum_{i=1}^{24} \dot{m}_{ew} \text{ Kg/m}^2 \cdot \text{day} \quad (22)$$

3.4. Mathematical solution

The solution of governing equations is tedious and time consuming. So, they are solved numerically using Matlab program. Governing equations Flow chart and Matlab code of mathematical model are presented in appendix A and B. Solving governing equations using Matlab can be predict solar still productivity at different climatic and design parameters presented in section 5.3.

CHAPTER (4)

AN EXPERIMENTAL STUDY

4.1 Experimental Set Up

The experimental set-up of the present work consists of the following components:

- Two identical solar stills. One of them is provided with a heat exchanger.
- Evacuated tube solar water heater.
- Flat plate solar water heater.
- Saline water tank.
- Hot water circulation pump.
- Control valves.

Detailed description of main components of the experimental setup is presented in the following pages.



Fig. 4.1: Experimental set-up

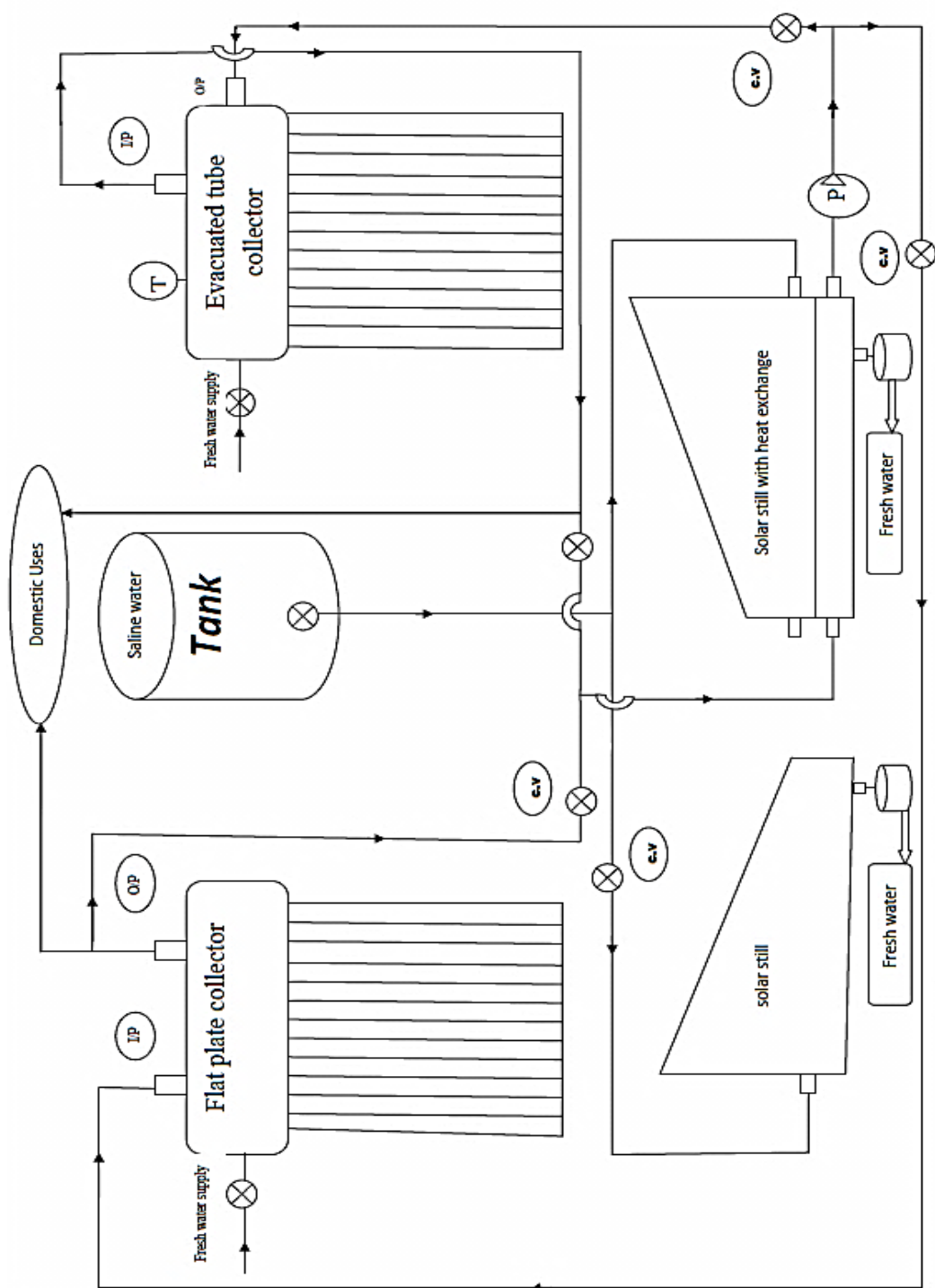


Fig. 4.2: Experimental set-up schemaic diagram

4.1.1 Solar still

The solar still under investigation are shown in figure 4.2. The greenhouse type solar stills have glass cover (5 mm thick) at an inclination angle 35° facing south. A rectangular trough is fixed at the downstream end of the slope cover for the collection of the distilled water which leads it to a collecting vessel. The still is filled early morning, and the day's production is collected at evening. Silicon rubber sealant is used to prevent leakage from any gap between the glass covers and the still box. The side walls and the base of the unit are insulated with cork (thermal conductivity = $0.035 \text{ W/m}^2 \text{ K}$) of 6 cm thick. The water depth inside the still is kept 2 cm at start of each experimental. The basin of the solar still is made water tight to avoid water leakage and the inside surface is blackened to absorb maximum solar radiation. It should probably be baked in the sun for a while before it is used in order to free the paint of any volatile toxicants which might otherwise evaporate and condense along with the drinking water. The bottom and sides of the basin are insulated to reduce the heat losses to the surrounding. A heat exchanger is provided directly under the basin of one still to heat the water in its basin as shown in figure 4.3. The heat exchanger dimensions are 62 cm long, 50 cm width, and 10 cm height. The main advantage of the basin heat exchanger is to add more energy to the still basin.

(a) (b)



Fig.4.3: (a) Solar still stand alone (b) Solar still with heat exchanger

4.1.2 Evacuated tube solar water heater

Figures 4.4 show the evacuated tube solar water heater. It will be connected with heat exchanger of the solar still. Characteristics and specification of the evacuated tube solar water heater as following:

Specification

Model: SP-TG58-1800

Length: 1800mm

Outer tube diameter: 58mm

Inner tube diameter: 47mm

Glass thickness: 1.5mm

Thermal expansion: 3.3×10^{-6} c

Material: borosilicate glass

Absorption coefficient: 96%

Emission coefficient: 4%

Vacuum: $p < 5 \times 10^{-3}$ pa

Output temperature: 95 c

Net weight: 2.23kg



Fig.4.4: Evacuated tube collector

Advantages

1. Glass tube perfectly overcomes the rusting problem from copper tube in other kind of solar water heater.
2. High production technology makes water to reaches 98°C in a very fast way which will in dead save the excessive use of hot water.
3. Premier stainless steel as inner tank can be well against rusting.
4. Provide 5 cm Polly urethane as insulation for keeping 24 hours long time hot water supply and the temperature loss will be less than 5°C .

4.1.3 Flat plate collector

Flat plate solar collectors showing in Figure4.5 have the following characteristics:

- Water tank capacity reach 150 liter.
- These collectors are better suited for moderate temperature
- Applications where the demand temperature is $30\text{-}70^{\circ}\text{C}$
- Consist of 10 hot water tube



Fig.4.5: Flat plate collector

4.1.4 Accessories

a. Hot water circulation pump

Circulation pump shown in Figures 4.1 and 4.6 have the following characteristics:

Manufactured by: Spain

Model: leader (R2S 15-40 MOD B)

Power: (73-47-33) W

RPM: (2500 - 2200- 1600)

Input volt: 230 V-50 HZ

Input current: (0.33-0.23-0.16) A

Class: class F (recirculation pump)



Fig.4.6: Recirculation pump.

4.2 Measurement Instrument Specification

The following is a list of all instruments and their specifications

4.2.1 Temperature sensors (Thermocouples with screw)

Model: thermocouple with screw Type k, (Refer to Figure 4.7)

Well Length: 100cm

Temperature Range: 0-600 C

Accuracy: $\pm 0.2^{\circ}\text{C}$



Fig.4.7: Temperature sensors (Thermocouple type K)

4.2.2 Temperature sensors (Thermocouples)

- 3mm diameter, 152.4mm (6") long probe sheath, (Refer to Figure 4.8)
- 310 Stainless Steel, mineral insulated probe sheath for high temperatures 1100°C (2012°F)
- Probe can be easily bent to desired shape
- Probe tip is ungrounded for maximum performance in electrically 'noisy' automotive environments.
- Stainless steel over-braid on a Teflon lead, resists abrasions and cuts, yet remains flexible.

- long 1 m (40") length lead.
- Spring strain relief prevents "pinching" of the lead wire.
- Miniature male K-type connector featuring a cable clamp.

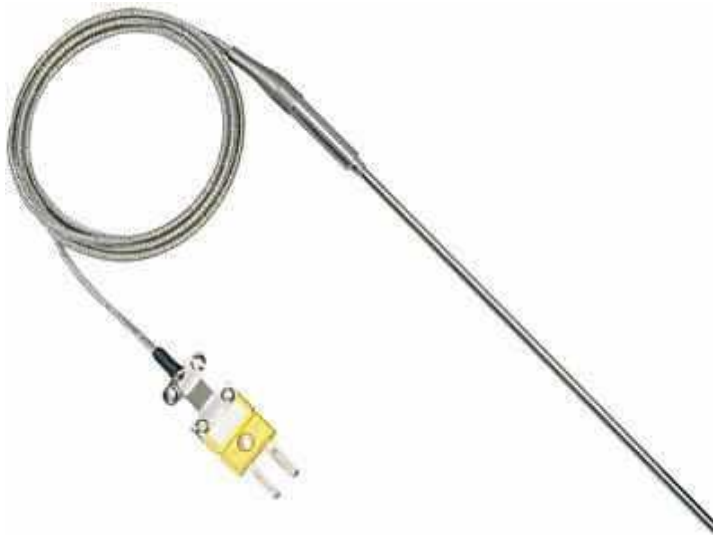


Fig.4.8: Temperature sensors (Thermocouple type K) measure glass temperature

4.2.3 Hanna thermocouple instrument

Table 4.1: Hanna thermocouple specification

Range	-200.0 to 999.9°C; 1000 to 1371°C; -328.0 to 999.9°F; 1000 to 2500°F
Resolution	0.1°C (-149.9 to 999.9°C); 0.2°C (-200.0 to -150.0°C); 1°C (outside) 0.1°F (-24.9 to 999.9°F); 0.2°F (-249.9 to -25.0°F); 0.3°F (-328.0 to -250.0°F); 1°F (outside)
Accuracy	±0.5°C (-100.0 to 999.9°C); ±0.1°C (outside); ±1°F (-148.0 to 999.9°F); ±0.15° (outside); (for 1 year, excluding probe error)
Probe	HI 766 series K-type thermocouple (not included)
Battery Type / Life	1.5V AA (3) / approximately 500 hours of continuous use (with backlight off); auto-off after 60 minutes of non-use (can be disabled)
Environment	-10 to 50°C (14 to 122°F); RH max 100%
Dimensions	150 x 80 x 36 mm (5.9 x 3.1 x 1.4")
Weight	235 g (8.3 oz.)



Fig.4.9: Hanna instrument for measuring glass temperature

4.2.4 Temperature Recorder (measure ambient temperature)

1. Temperature-Humidity Sensor
2. LCD Display
3. ON/OFF/HOLD switch
4. Temperature units switch (°C & °F)
5. Temperature/Humidity/Record switch
6. RECORD / ERASE button (Model 446580 only)
7. Wet bulb calibration adjustment (for factory use only)
8. Dry bulb calibration adjustment (for factory use only)

The battery compartment and the tripod mount are located on the rear of the instrument.

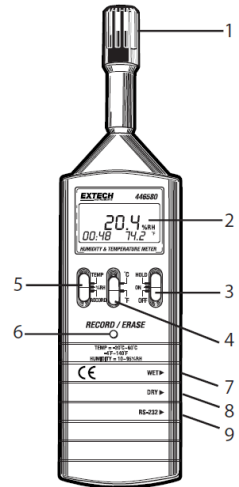


Fig.4.10:Temperature recorder

General Specifications

Display: Multi-function 3 ½ digit (2000 count) LCD display

Measurement: Relative Humidity% (RH) and Temperature (°C & °F)

Data Hold: Freezes Display Data logger (446580) Records approx. 7000 readings

Data Output 446580: Analog 10mVDC per °C/F or %RH

Response Time Humidity: 45% to 95%: ≤ 3 minutes, 95% to 45%: ≤ 5 minutes

Measurement rate: 2.5 readings per second

Operating Temperature: 32 to 122°F (0 to 50 °C)

Operating Humidity < 80% RH

Storage Temperature: 14 to 140°F (-10 to 60°C)

Storage Humidity < 70% RH

Power Supply: 9V battery

Battery life: 400 hours

Weight: 7.0 oz. (198 g)

Size 10.6 x 2.7 x 1.0" (180 x 72 x 32mm)

Accuracy: ($\pm 0.8^{\circ}\text{C}$)



Fig.4.11:Temperature recorder

4.2.5 Haenni solar intensity Recorder

Manufactured by: Haenni. Co, Figure 4.13

Model: solar 118

Wire Length: 400cm

Radiation Range: 0-1500 W/m^2

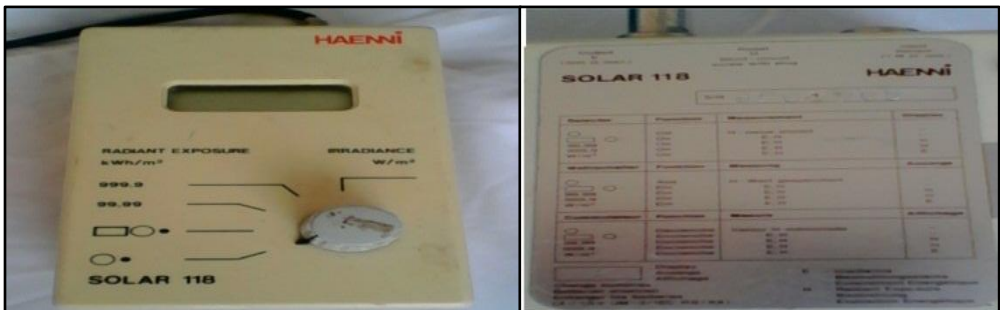


Fig.4.12:Haenni solar radiation



Fig.4.13:Sensor of solar radiation

CHAPTER (5)

RESULTS AND DISCUSSION

5.1. Introduction

In this work experimental investigation has been carried on a similar still coupled to a flat plate collector and evacuated tube collector. The system was operated continuously for several months (April to august) under different climatic conditions, covering months with moderate and high sunshine. Weather conditions collected through April to August were used for validation of the mathematical model, while data collected for January, March, were used to predict the solar still productivity during the winter days. Investigations were targeted to enhance the still output through improving its operating condition by using a flat plate collector FPC and evacuated tube collector ETC. The temperatures of brackish water, glass covers, and meteorological condition are recorded continuously. Open loop experiments were designed to enable us using hot water leaving heat exchanger in the domestic applications. Experiments show that using open loops is not usefully and solar still productivity decreases. On the other hand closed loop experiments show that solar still productivity enhanced when used ETC. Numerical and experimental results are presented in table C.1, C.2, C.3 and C.4, refer to Appendix C.

5.2. Comparison Between Passive Solar Still And Active Solar Still

5.2.1 Open loop test

A. Solar still with flat plate collector FPC, (June 11th, 2014)

The variations of the ambient temperature and the solar radiation for a typical day in summer season are shown in Figure 5.1. The figure shows that highest temperatures occurred between the hours of 13–14 p.m.

also the ambient temperatures ranges were between 31.5 and 40°C. The variation of the water temperature in standalone solar still and solar still coupling with a solar water heater is shown in Figure 5.2.

The output temperature from heat exchanger will be higher than input temperature because of absorbing heat from water in basin. The percentage of enhancement in daily productivity due to coupling of solar collector with open cycle decreased. Figure 5.4 shows that the daily productivity of active solar still is 1.56 liter while the productivity of passive solar still is 1.8 liter. The productivity of active solar still is lower 14% than passive solar still. Figure 5.3 shows comparison between theoretical and experimental results of glass temperature. In the first three hours. The glass temperature in active solar still is higher than the glass temp in passive solar still due to the raising in the water temperature in solar still coupled with solar water heater. After three hours glass temperature in a passive solar still will be higher than active solar still.

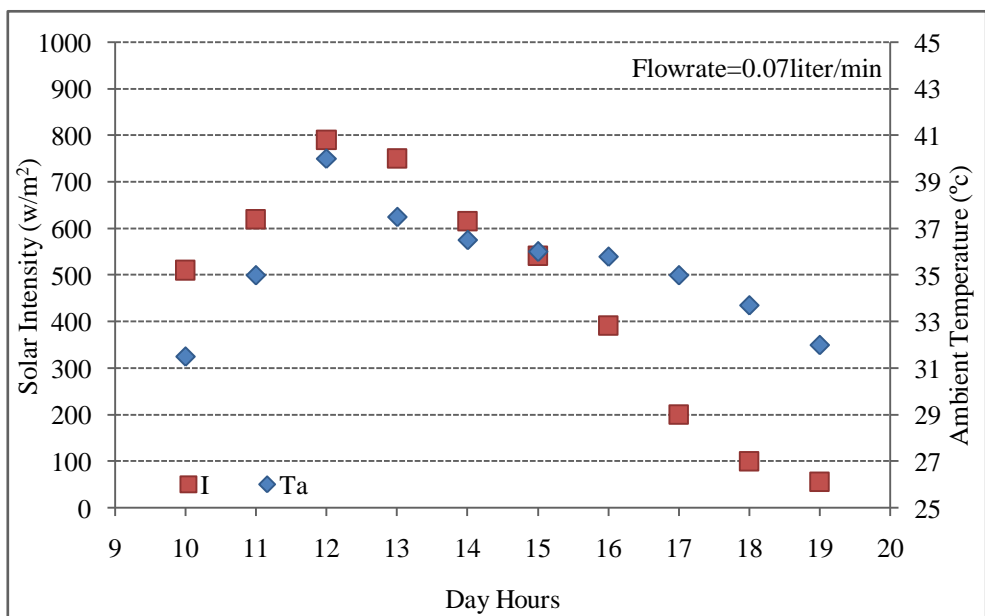


Fig.5.1: Hourly variation of solar intensity and ambient temperature, FPC (June 11th, 2014).

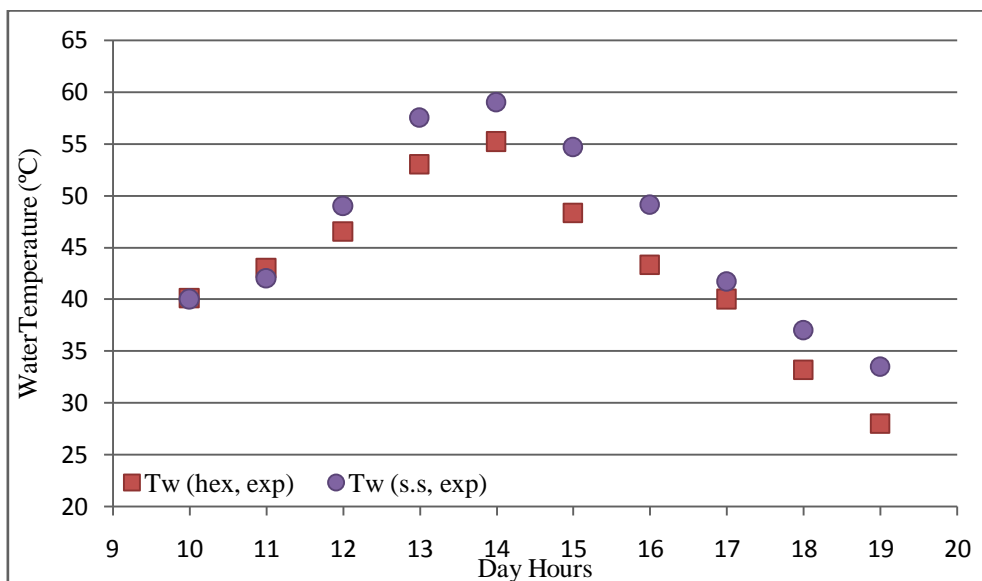


Fig.5.2: Comparison between experimental results of water temperature for FPC and standalone solar still, (June 11th, 2014).

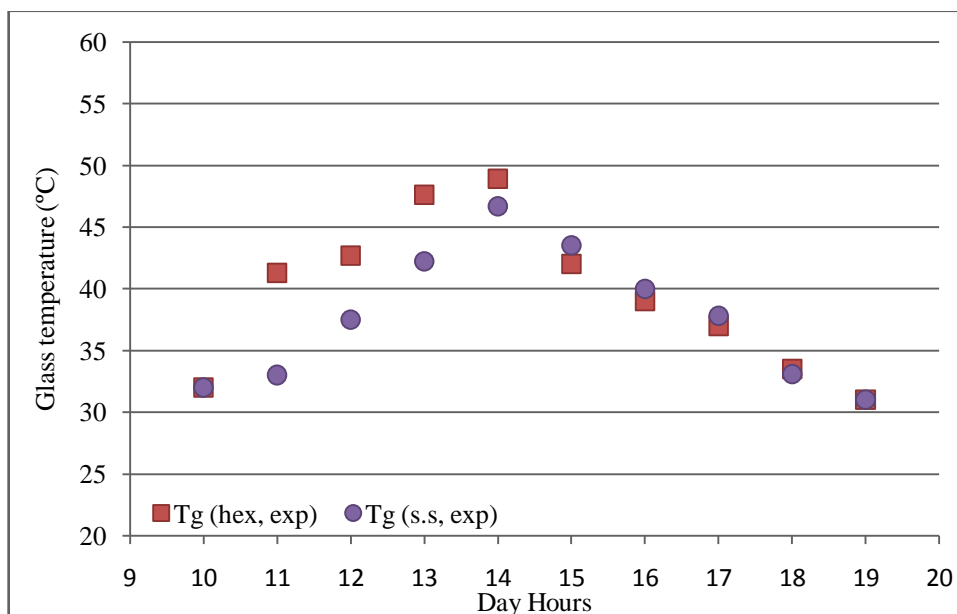


Fig.5.3: Comparison between experimental results of glasstemperature for FPC and standalone solar still, (June 11th, 2014).

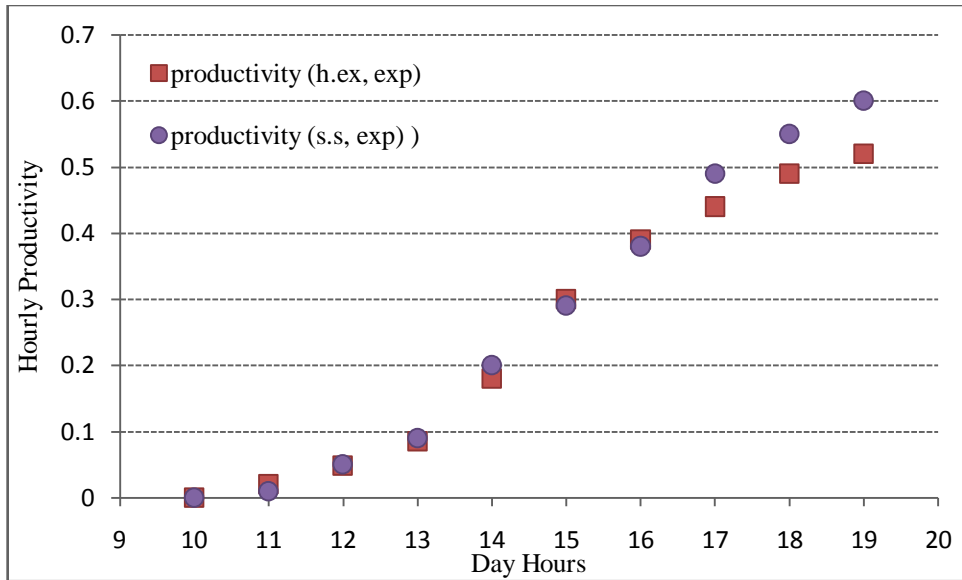


Fig.5.4: Comparison between experimental accumulated productivity for FPC and standalone solar still, (June 11th, 2014).

B. Solar still with evacuated tube collector ETC, (June 10th, 2014)

The variations of the ambient temperature and the solar radiation for a typical day in summer season are shown in Figure 5.5. The figure shows that highest temperatures occurred between the hours of 13–14 p.m. also the ambient temperatures ranges were between 28 and 38.5°C. The variation of the water temperature in standalone solar still and solar still coupling with a solar water heater is shown in Figure 5.6.

The output temperature from heat exchanger will be higher than input temperature because of absorbing heat from water in basin. The percentage of enhancement in daily productivity due to coupling of solar collector with open cycle decreased. Figure 5.8 shows that the daily productivity of active solar still is 1.65 liter while the productivity of passive solar still is 2.04 liter. The productivity of active solar still is lower 20% than passive solar still. Figure 5.7 shows comparison between theoretical and

experimental results of glass temperature. In the first three hours. The glass temperature in active solar still is higher than the glass temp in passive solar still due to the raising in the water temperature in solar still coupled with solar water heater. After three hours glass temperature in a passive solar still will be higher than active solar still.

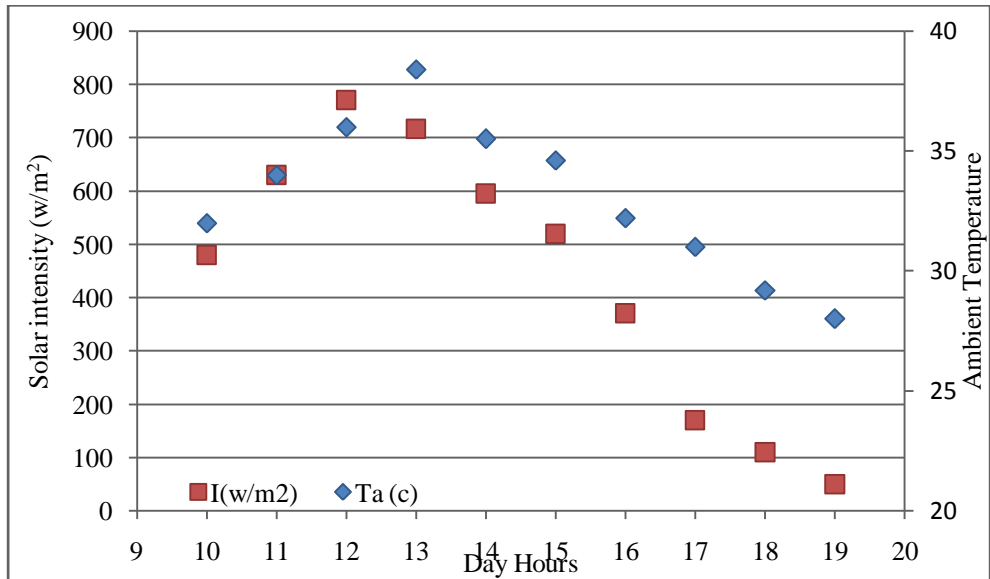


Fig.5.5: Hourly variation of solar intensity and ambient temperature, ETC (June 10th, 2014).

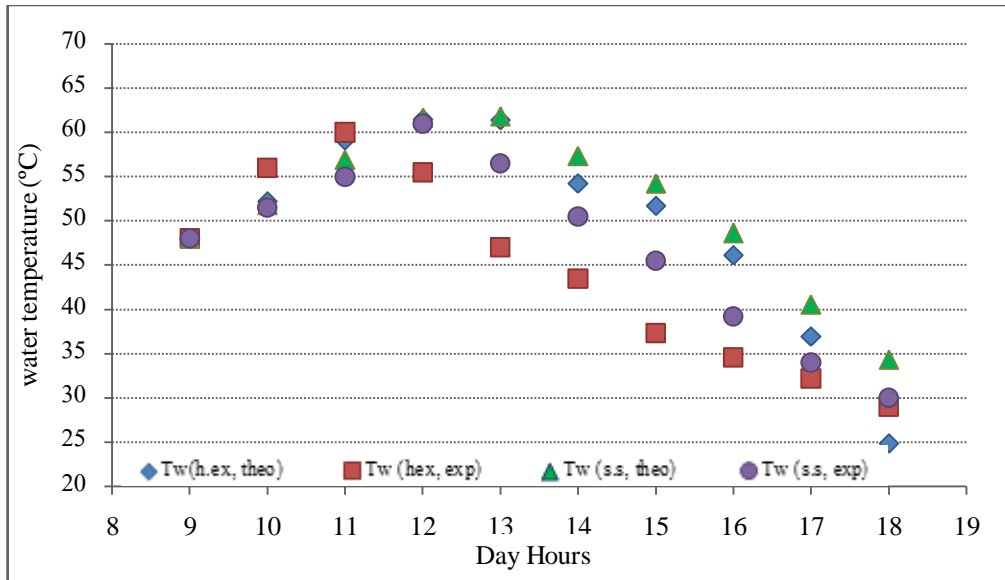


Fig.5.6: Comparison between theoretical and experimental results of water temperature for ETC and standalone solar still, (June 10th, 2014).

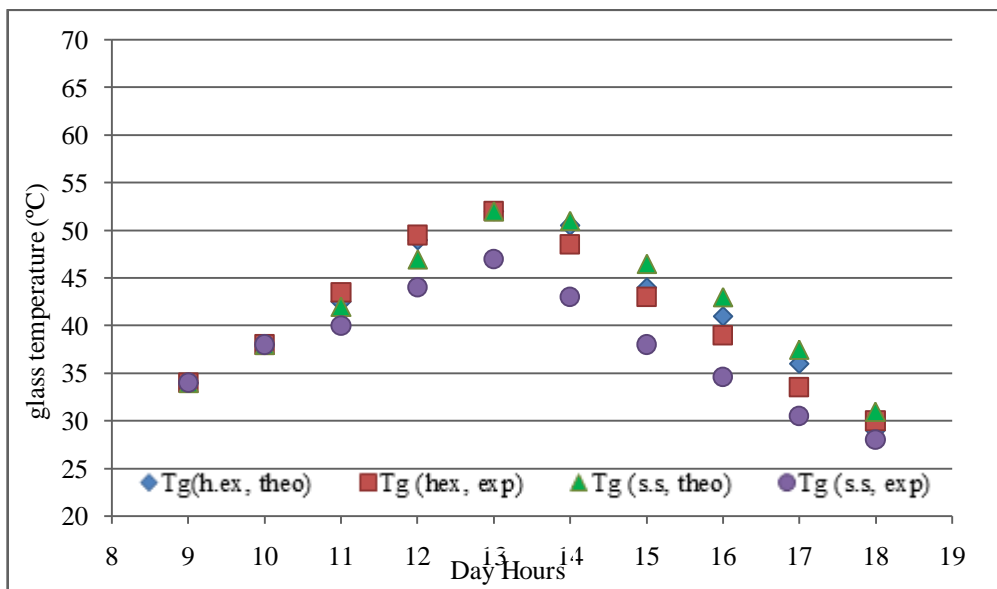


Fig.5.7: Comparison between theoretical and experimental results of glass temperature for ETC and standalone solar still, (June 10th, 2014).

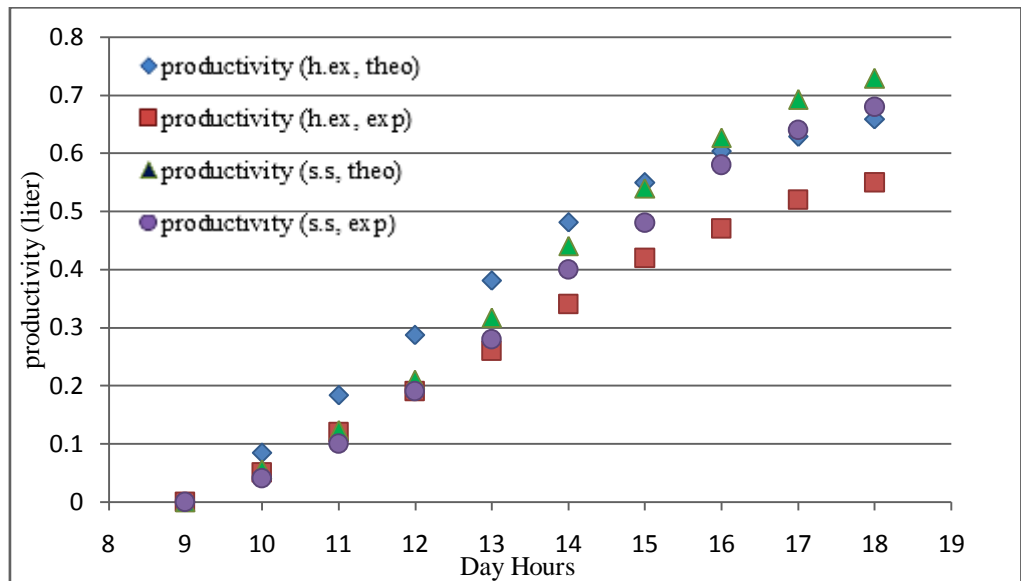


Fig.5.8: Experimental and theoretical accumulated productivity forETC and standalone solar still, (June 10th, 2014).

C. Solar still with evacuated collectorETC, (June 16th, 2014).

The variations of the ambient temperature and the solar radiation for a typical day in summer season are shown inFigure 5.9. The figure shows that highest temperatures occurred between the hours of 13–14 p.m. also the ambient temperatures ranges were between 33 and 46.5°C. The variation of the water temperature in standalone solar still and solar still coupling with a solar water heater is shown in Figure 5.10.

The output temperature from heat exchanger will be higher than input temperature because of absorbing heat from water in basin. The percentage of enhancement in daily productivity due to coupling of solar collector with open cycle decreased. Figure 5.12 shows that the daily productivity of active solar still is 1.1 liter while the productivity of passive solar still is 2.4 liter. The productivity of active solar still is lower 55% than

passive solar still. Figure 5.11 shows comparison between theoretical and experimental results of glass temperature. In the first three hours. The glass temperature in active solar still is higher than the glass temp in passive solar still due to the raising in the water temperature in solar still coupled with solar water heater. After three hours glass temperature in a passive solar still will be higher than active solar still.

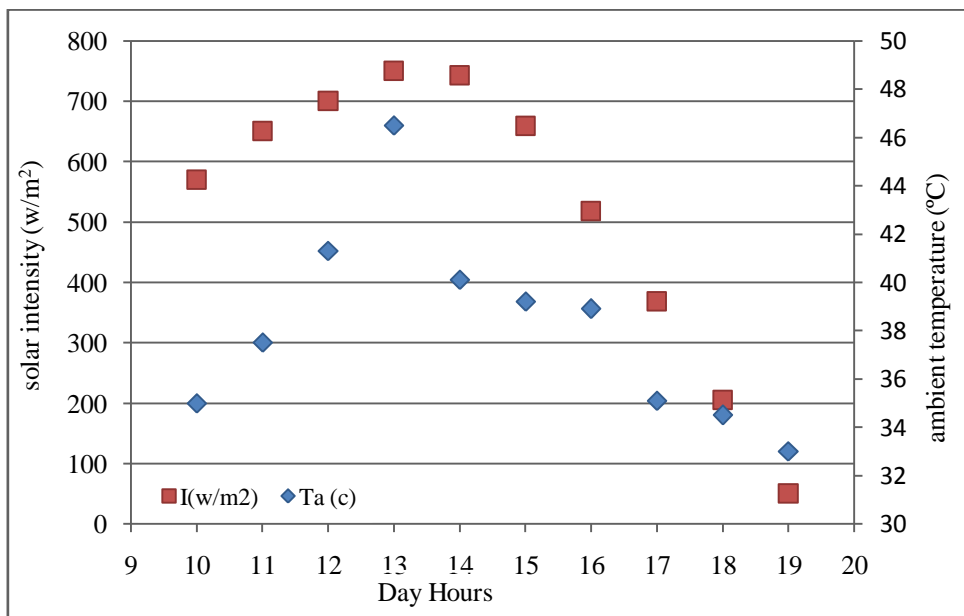


Fig.5.9: Hourly variation of solar intensity and ambient temperature, ETC (June 16th, 2014).

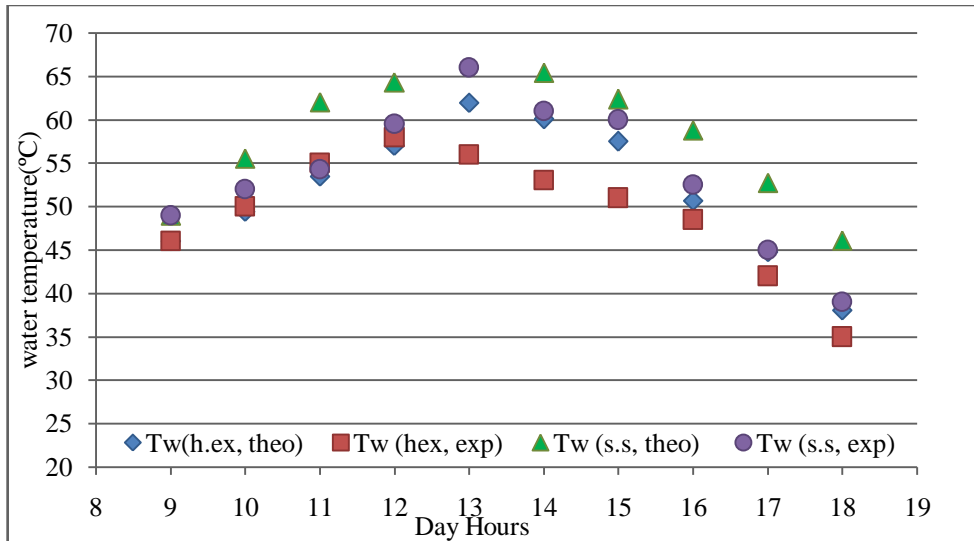


Fig.5.10: Comparison between theoretical and experimental results of water temperature for ETC and standalone solar still, (June 16th, 2014).

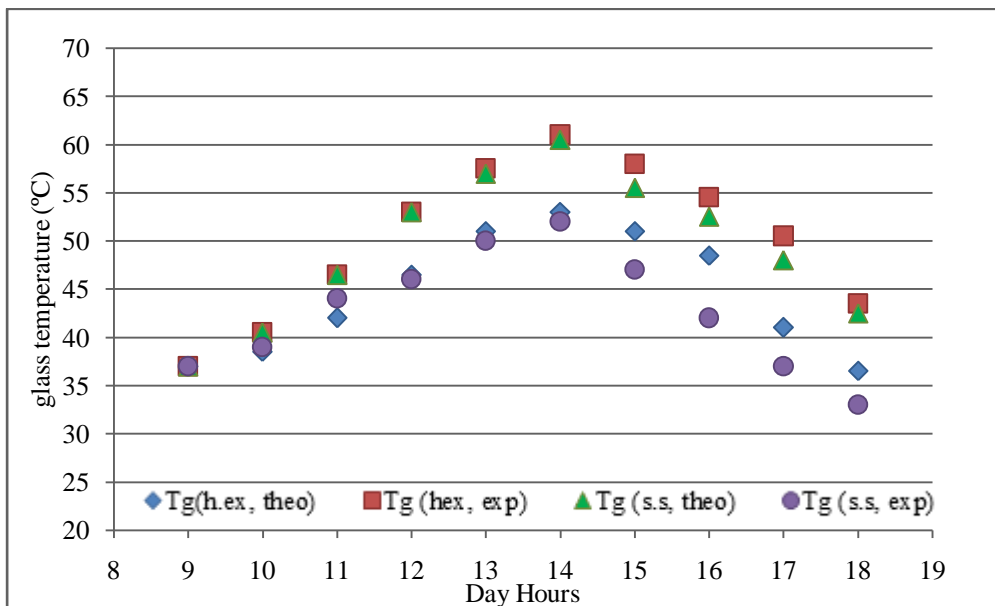


Fig.5.11: Comparison between theoretical and experimental results of glass temperature for ETC and standalone solar still, (June 16th, 2014)

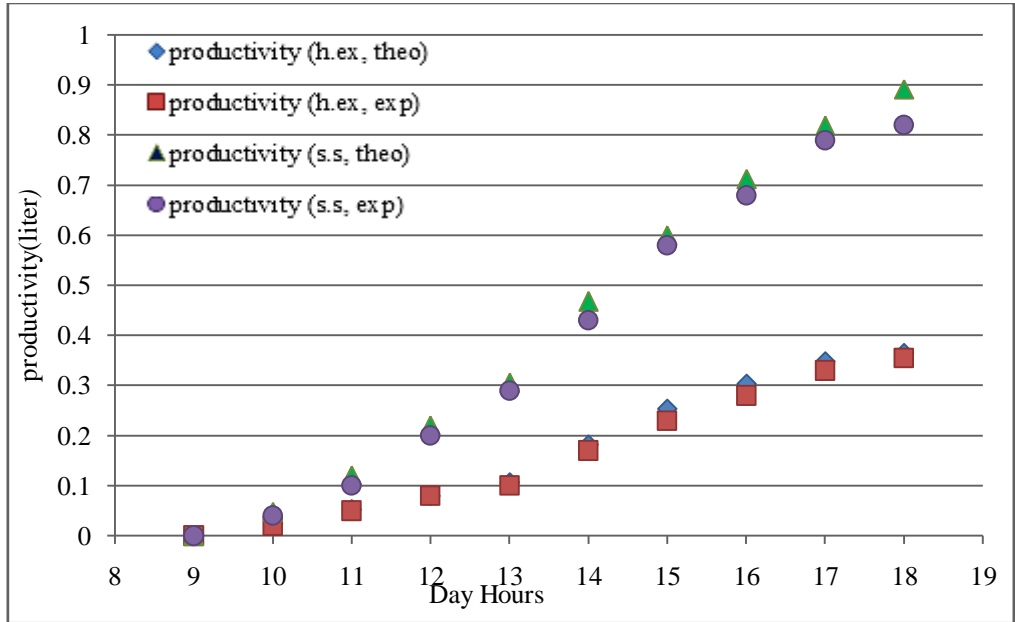


Fig.5.12: Experimental and theoretical accumulated productivity for ETC and standalone solar still, (June 16th, 2014)

The previous three cases show that in open loop experiment the first three hours water temperature in solar still coupled with solar water heater is higher than water temperature in a passive solar still. Due to higher water temperature in a solar still coupling with solar water heater, distilled water obtained is more than standalone solar still. Moreover, after three hours the water temperature in a passive solar still rising than active solar still consequently higher output from standalone solar still will be obtained. High productivity in first three hours in active solar still is a result of coupling solar water heater, due to outlet hot water from solar water heater to heat exchanger. Increasing water temperature in the basin increase the evaporation rate, consequently increasing the productivity as well as the total output of distillate. Once the output temperature from solar water heater becomes lower than water temperature in basin the heat will be transfer from water in the basin to water in the heat exchanger and the productivity will be decreased. So that the open loop cannot be used.

5.2.2 Closed loop test

A. Solar still with flat plate collector FPC (June 17th, 2014).

The variations of the ambient temperature and the solar radiation for a typical day in summer season are shown in Figure 5.13. The figure shows that highest temperatures occurred between the hours of 13–14 p.m. also the ambient temperatures ranges were between 39 and 44°C. The variation of the water temperature in standalone solar still and solar still coupling with a solar water heater is shown in Figure 5.14.

In the first three hours water temperature in solar still coupled with solar water heater is higher than water temperature in a passive solar still. Due to higher water temperature in a solar still coupling with solar water heater, distilled water obtained is more than standalone solar still. Moreover, after three hours the water temperature in a passive solar still rising than active solar still consequently higher output from standalone solar still will be obtained.

This high productivity in first three hours in active solar still is a result of coupling solar water heater, due to outlet hot water from solar water heater to heat exchanger, water temperature increase in the basin and increase the evaporation rate, consequently increasing the productivity as well as the total output of distillate, until the output temperature from solar water heater is lower than water temperature in basin so the heat will be transfer from water in the basin to water in the heat exchanger and the productivity will be decreased until stopping.

The output temperature from heat exchanger will be higher than input temperature because of absorbing heat from water in basin. The percentage of enhancement in daily productivity due to coupling of solar collector with open cycle decreased. Figure 5.16 shows that the daily productivity of active solar still is 1.56 liter while the productivity of passive so-

lar still is 2.28 liter. The productivity of active solar still is lower 32% than passive solar still. Figure 5.15 shows comparison between theoretical and experimental results of glass temperature. In the first three hours. The glass temperature in active solar still is higher than the glass temp in passive solar still due to the raising in the water temperature in solar still coupled with solar water heater. After three hours glass temperature in a passive solar still will be higher than active solar still.

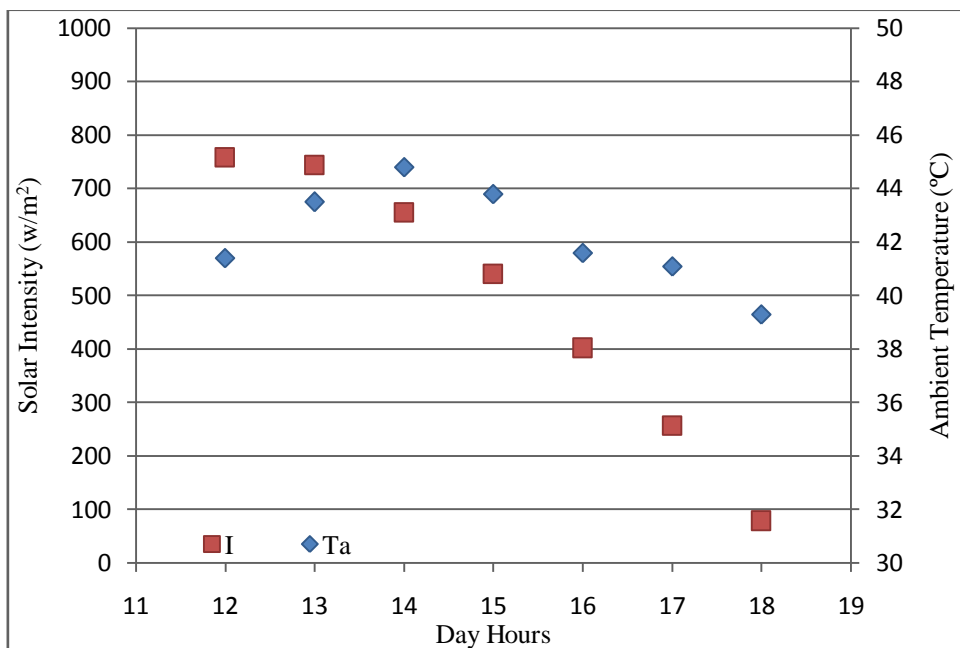


Fig.5.13: Hourly variation of solar intensity and ambient temperature, FPC (June 17th, 2014)

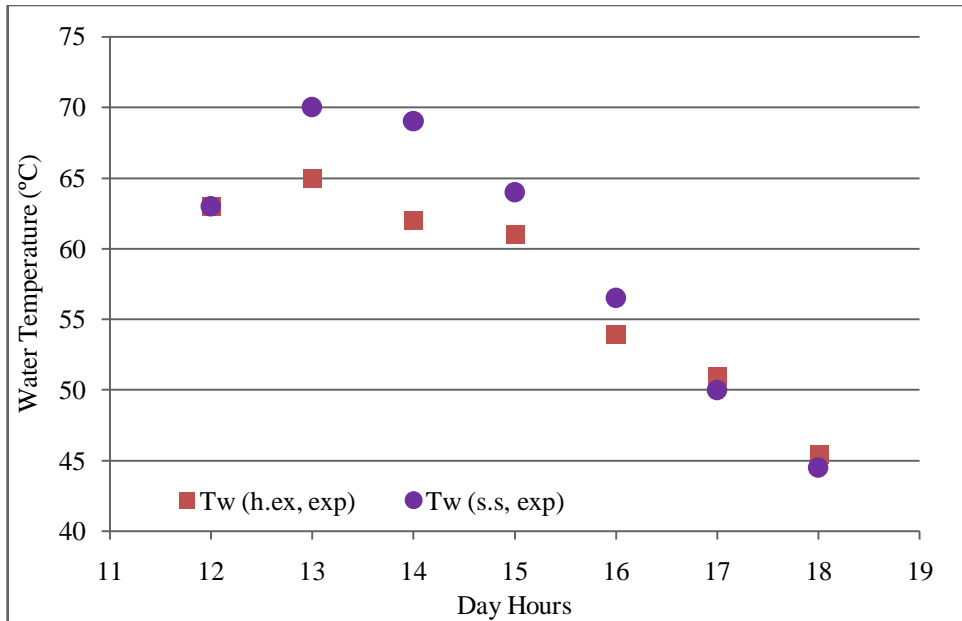


Fig.5.14: Comparison between experimental results of watertemperature for FPC and standalone solar still, (June 17th,2014).

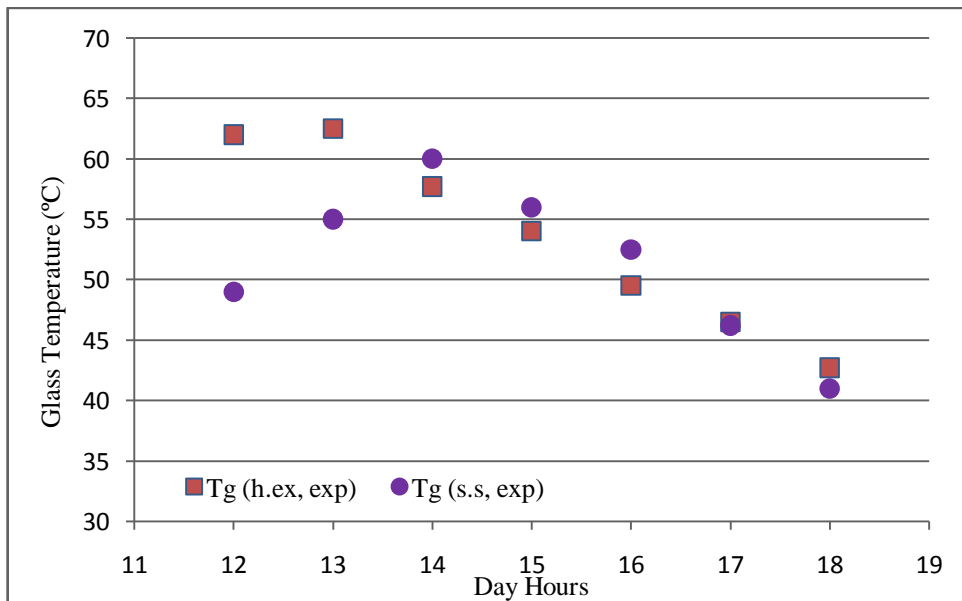


Fig.5.15: Comparison between experimental results of glass temperature for FPC and standalone solar still, (June 17th, 2014)

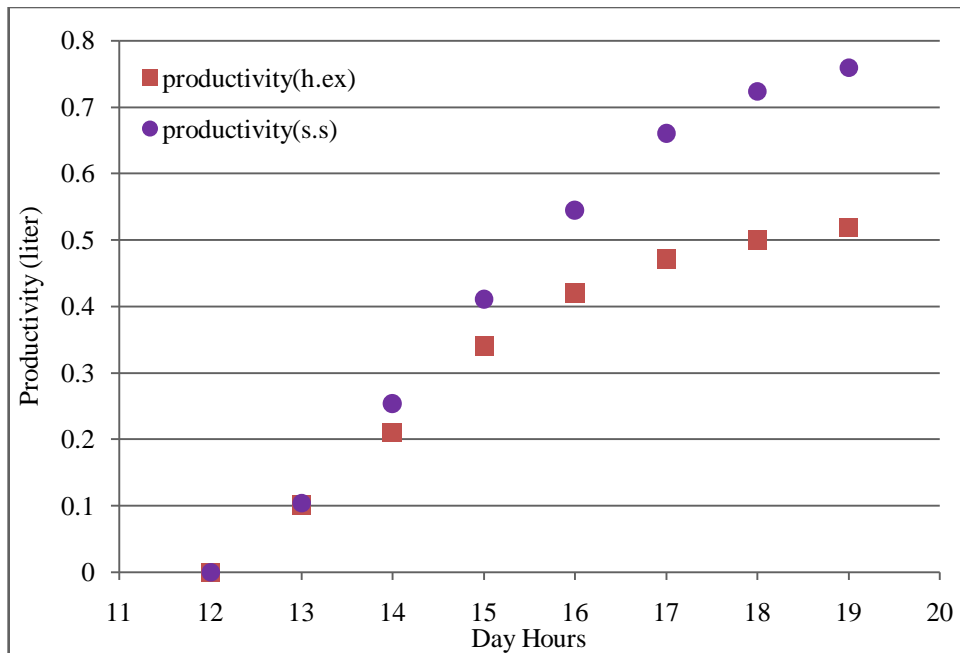


Fig.5.16: Experimental accumulated productivity for FPC and standalone solar still, (June 17th, 2014)

B. Solar still with evacuated tube collector ETC (Date 9 July 2014)

The variations of the ambient temperature and the solar radiation for a typical day in summer season are shown in Figure 5.17. The figure shows that highest temperatures occurred between the hours of 13–14 p.m. also the ambient temperatures ranges were between 37 and 41°C. The variation of the water temperature in standalone solar still and solar still coupling with a solar water heater is shown in Figure 5.18.

Water temperature in solar still coupled with solar water heater is higher than water temperature in a passive solar still. Due to higher water temperature in a solar still coupling with solar water heater, distilled water obtained is more than standalone solar still.

This high productivity in active solar still is a result of coupling solar water heater, due to outlet hot water from solar water heater to heat exchanger, water temperature increase in the basin and increase the evapo-

ration rate, consequently increasing the productivity as well as the total output of distillate

The percentage of enhancement in daily productivity due to coupling of solar collector with closed cycle increased. Figure 5.20 shows that the daily productivity of active solar still is 5.55 liter while the productivity of passive solar still is 2.16 liter. The productivity of active solar still is more 256% than passive solar still. Figure 5.19 shows comparison between theoretical and experimental results of glass temperature. The glass temperature in active solar still is higher than the glass temp in passive solar still due to the raising in the water temperature in solar still coupled with solar water heater.

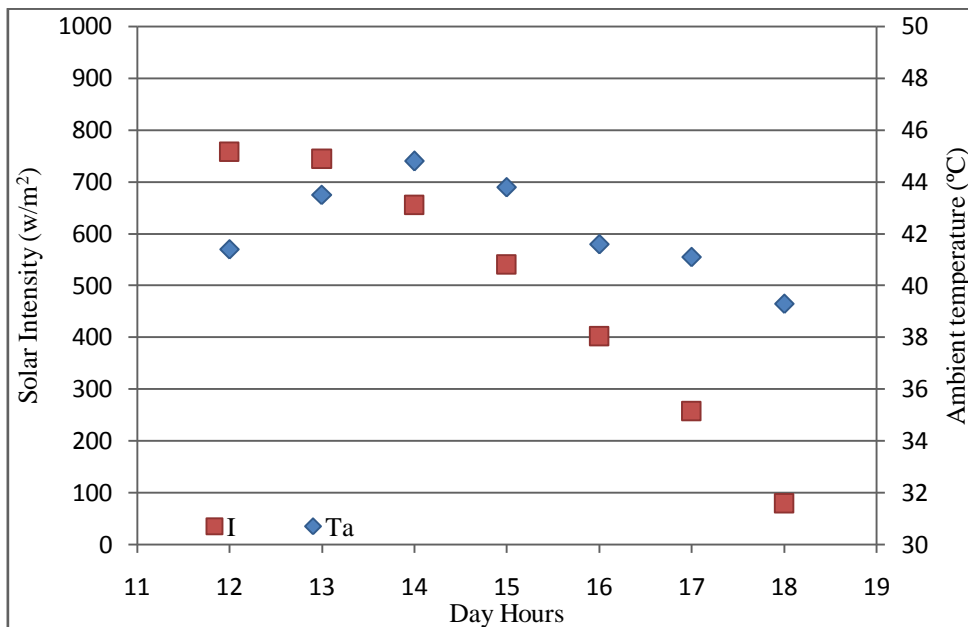


Fig.5.17:Hourly variation of solar intensity and ambient temperature, ETC (July 9,2014)

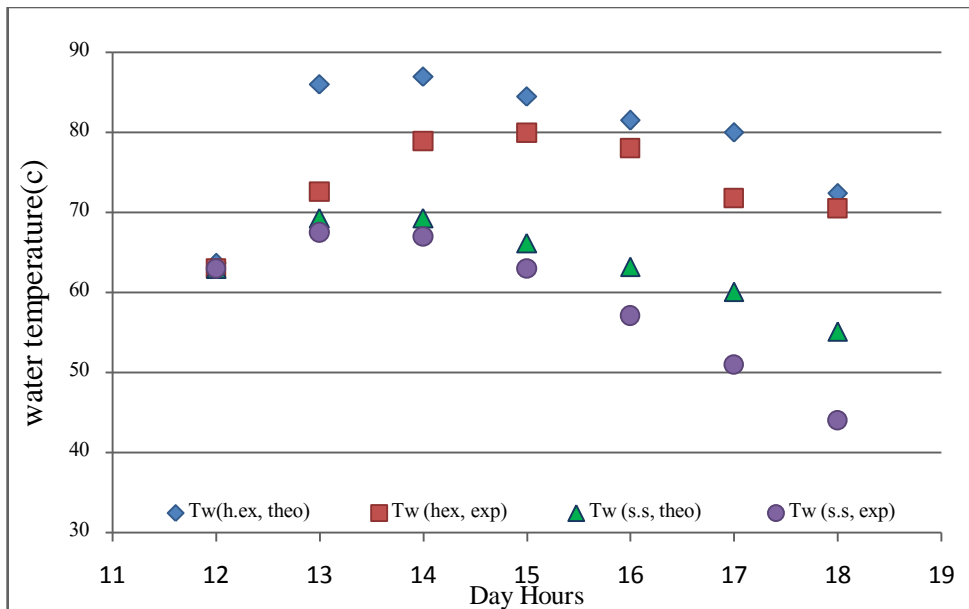


Fig.5.18: Comparison between theoretical and experimental results of water-temperature for ETC standalone solar still, (July 9,2014)

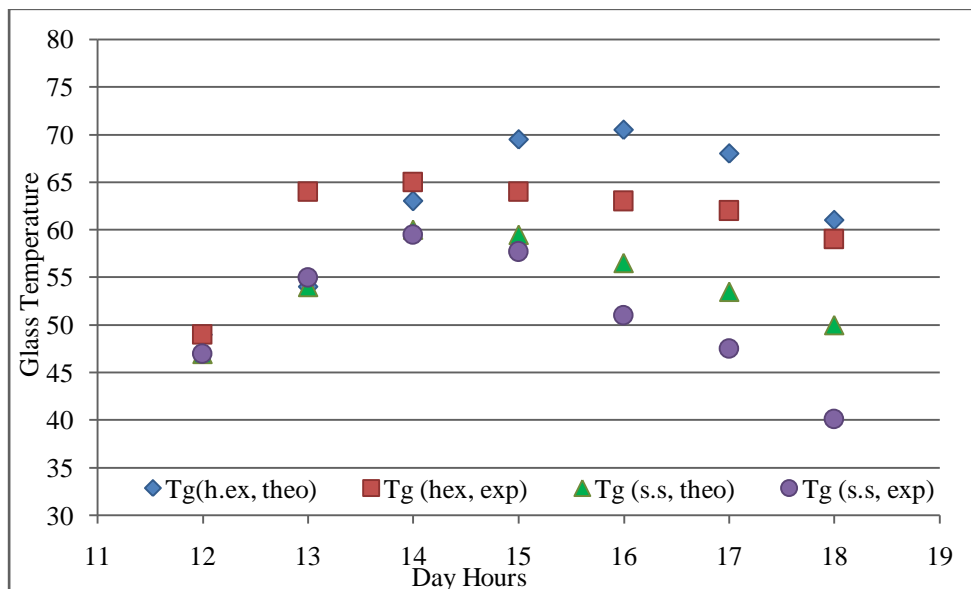


Fig.5.19: Comparison between theoretical and experimental results of glass temperature for ETC and standalone solar still, (July 9,2014)

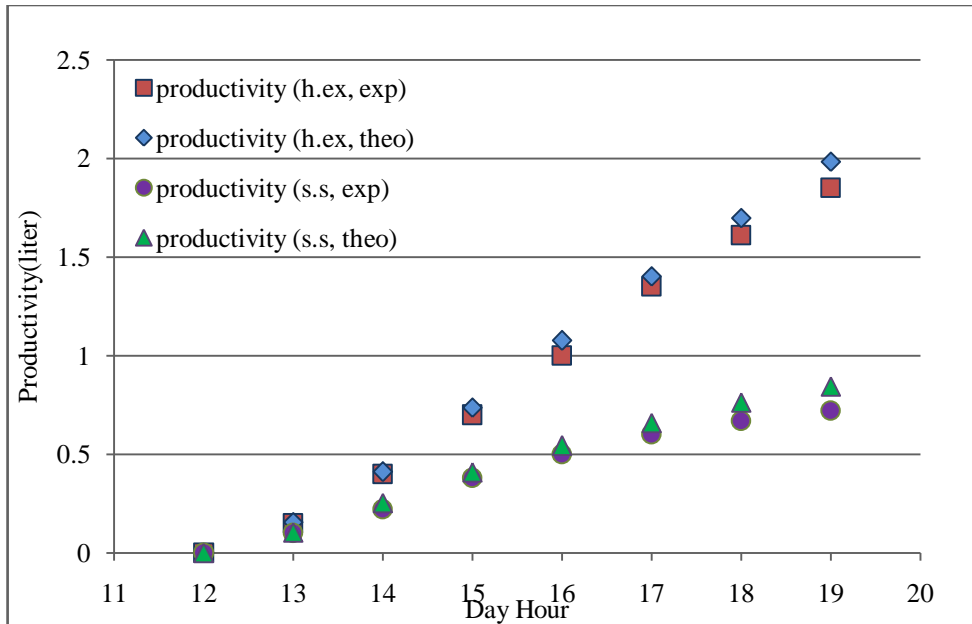


Fig.5.20: Experimental and theoretical accumulated productivity (July 9, 2014)

C. Solar still with evacuated tube collector ETC(August 9, 2014)

The variations of the ambient temperature and the solar radiation for a typical day in summer season are shown in Figure 5.21. The figure shows that highest temperatures occurred between the hours of 13–14 p.m. also the ambient temperatures ranges were between 28 and 42°C. The variation of the water temperature in standalone solar still and solar still coupling with a solar water heater is shown in Figure 5.22.

Water temperature in solar still coupled with solar water heater is higher than water temperature in a passive solar still. Due to higher water temperature in a solar still coupling with solar water heater, distilled water obtained is more than standalone solar still.

This high productivity in active solar still is a result of coupling solar water heater, due to outlet hot water from solar water heater to heat

exchanger, water temperature increase in the basin and increase the evaporation rate, consequently increasing the productivity as well as the total output of distillate

The percentage of enhancement in daily productivity due to coupling of solar collector with closed cycle increased. Figure 5.24 shows that the daily productivity of active solar still is 6.75 liter while the productivity of passive solar still is 2.46 liter. The productivity of active solar still is more 275% than passive solar still. Figure 5.23 shows comparison between theoretical and experimental results of glass temperature. The glass temperature in active solar still is higher than the glass temp in passive solar still due to the raising in the water temperature in solar still coupled with solar water heater.

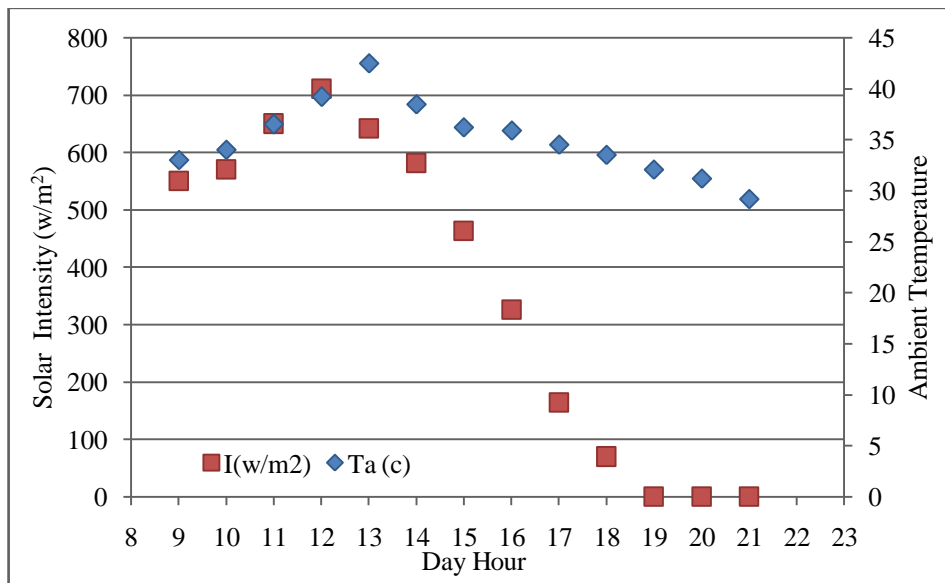


Fig.5.21:Hourly variation of solar intensity and ambient temperature in (August 9, 2014)

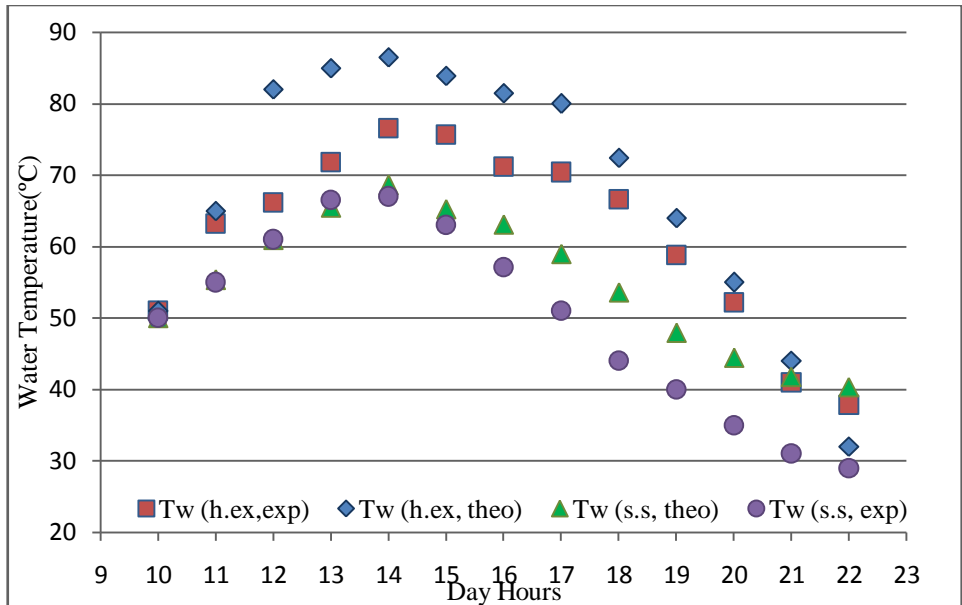


Fig.5.22: Comparison between theoretical and experimental results of wattertemperature, ETC (August 9, 2014)

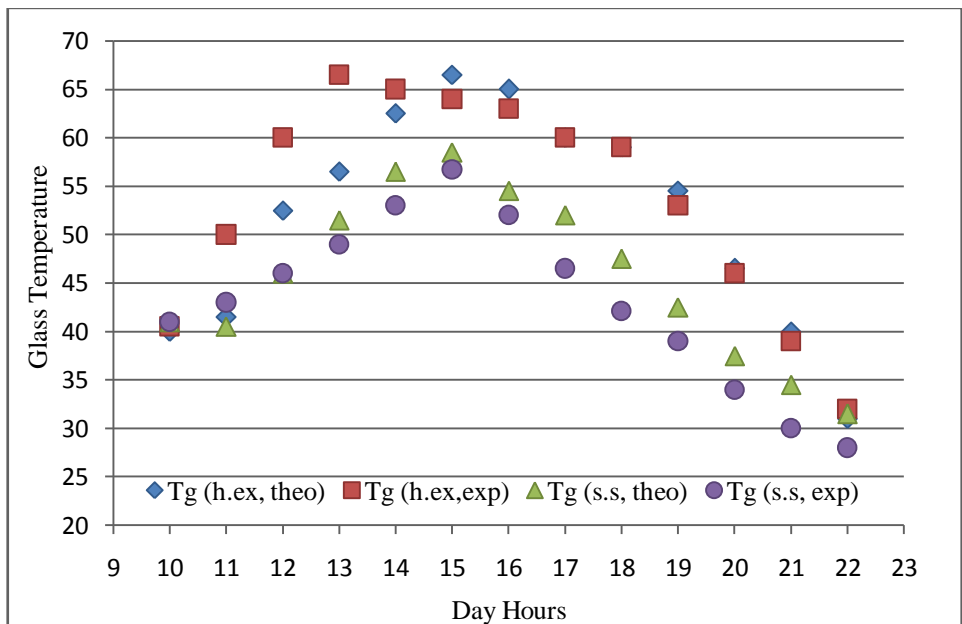


Fig.23:Comparison between theoretical and experimental results of glass temperature, ETC (August 9, 2014)

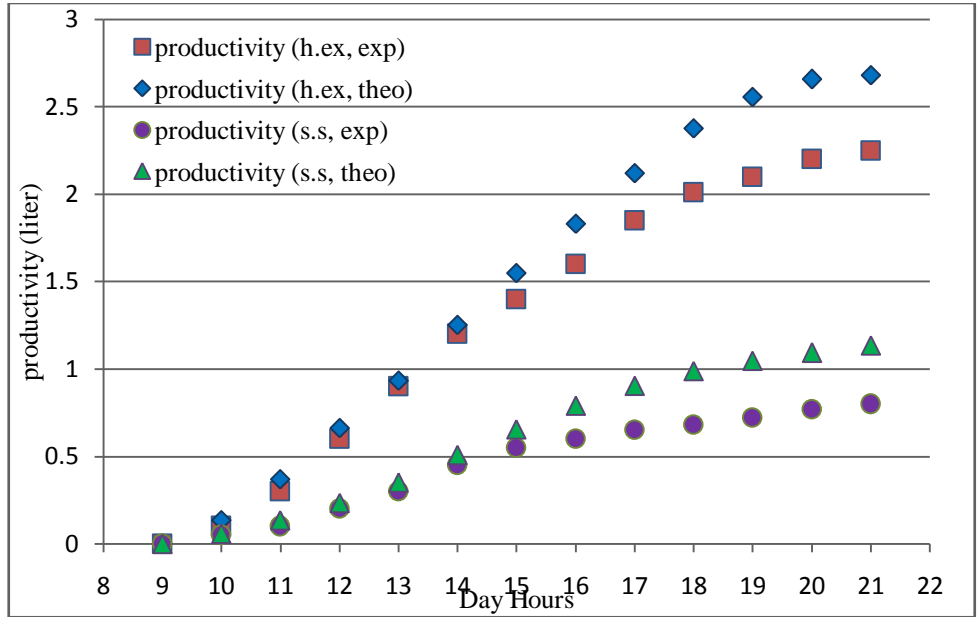


Fig.24: Experimental and theoretical accumulated productivity for ETC and standalone solar still, (August 9, 2014)

5.3. Numerical Result

Due to good agreement of the theoretical analysis,(Matlab program) with those of the experimental setup. Productivity for solar still could be predicted as well as its performance for large scale model under different working conditions. Figure 25 to 32 represent two different case studies in January and March. Results show that the productivity varies from $1.0 \text{ L/m}^2/\text{day}$ in January to $3.0 \text{ L/m}^2/\text{day}$ in March in Suezgovernorate.

A. Solar still with evacuated tube collector ETC(January 23, 2016)

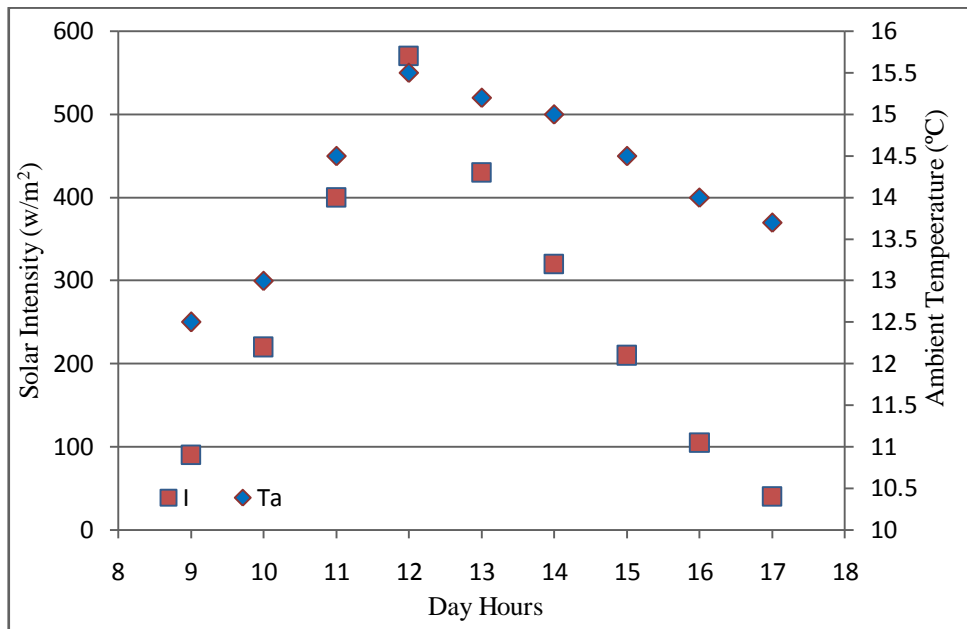


Fig.5.25:Hourly variation of solar intensity and ambient temperature,(January23, 2016)

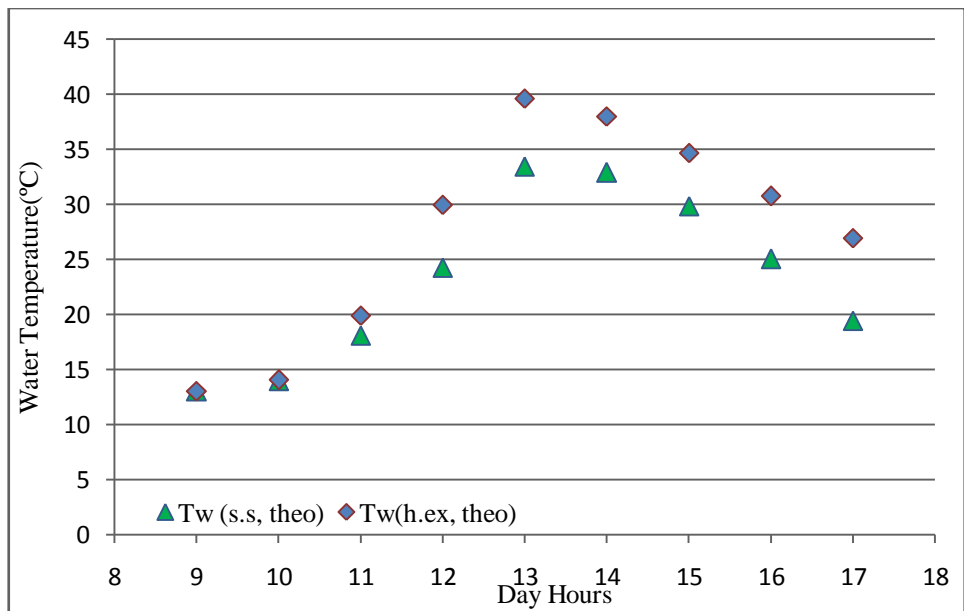


Fig .5.26: Theoretical results of water temperature for ETC and standalone solar still, (January23, 2016)

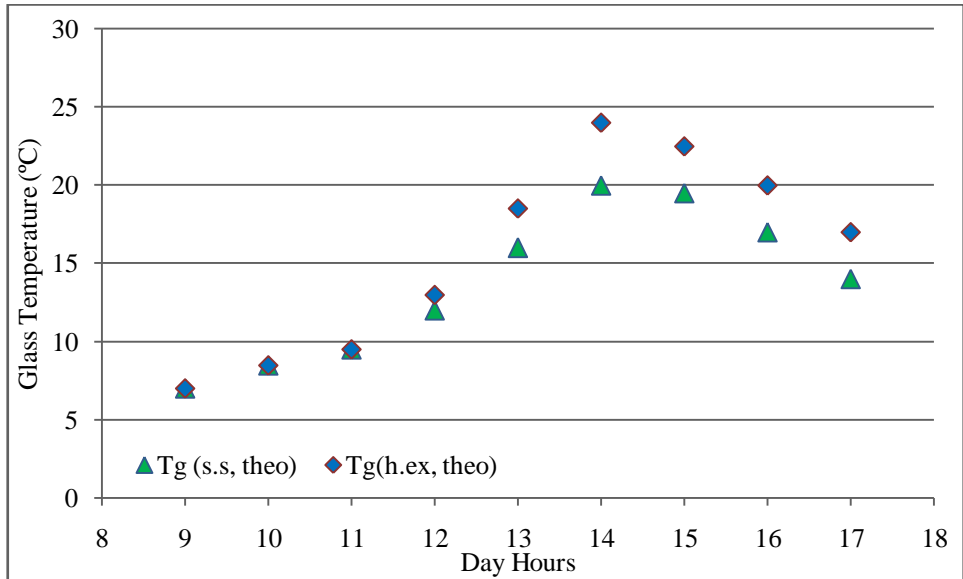


Fig .5.27: Theoretical results of glass temperature forETC and standalone solar still, (January23, 2016)

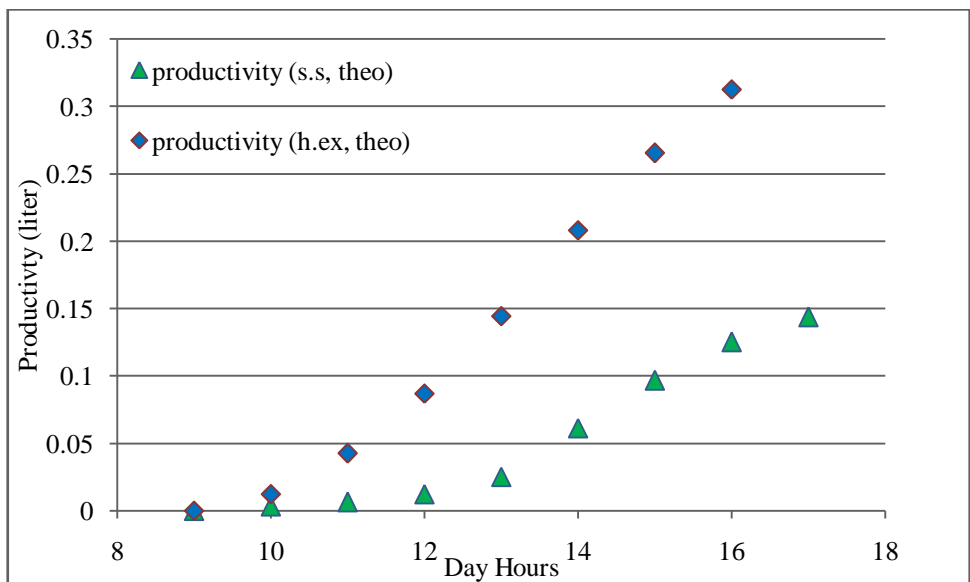


Fig .5.28: Theoretical accumulated productivity for ETC and standalone solar still, (January23, 2016)

B. Solar still with evacuated tube collector ETC(Mar 20, 2016)

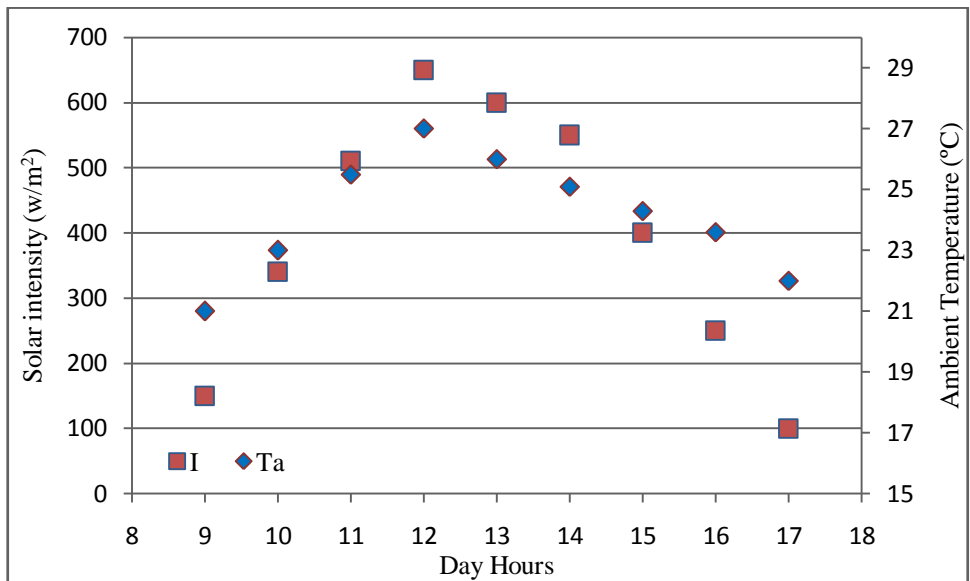


Fig.5.29:Hourly variation of solar intensity and ambient temperature, (March20, 2016)

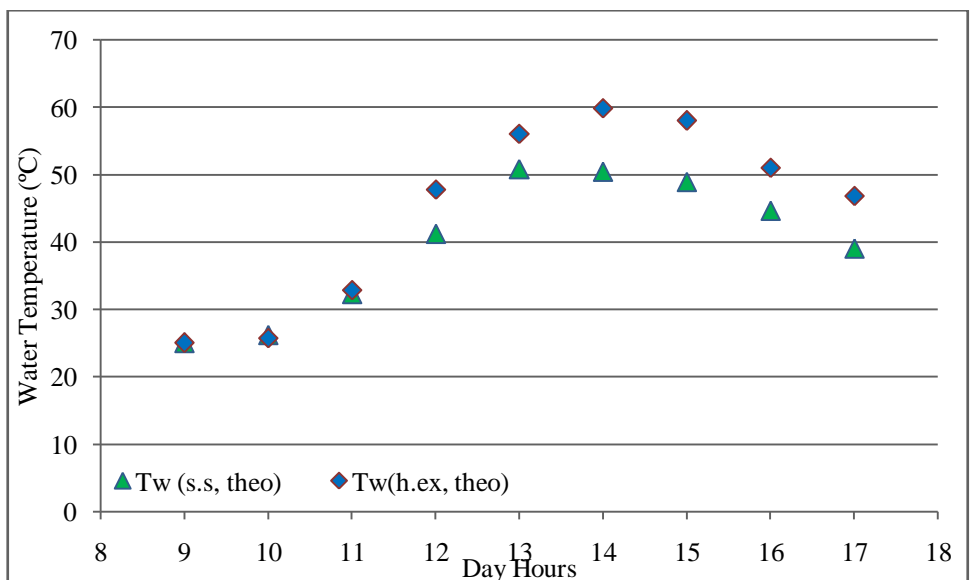


Fig .5.30: Theoretical results of water temperature for ETC and standalone solar still, (March20, 2016)

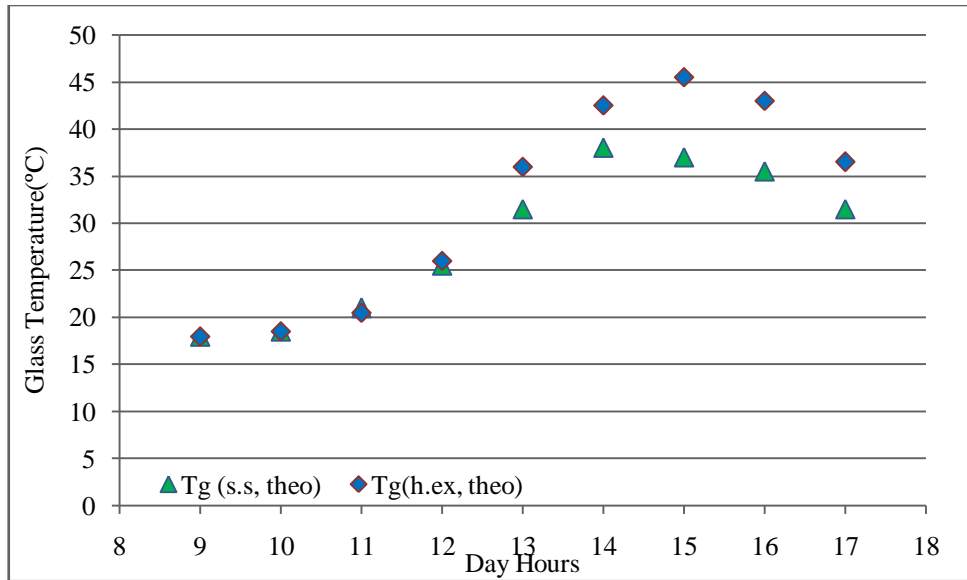


Fig .5.31: Theoretical results of glass temperature for ETC and standalone solar still,(March20, 2016)

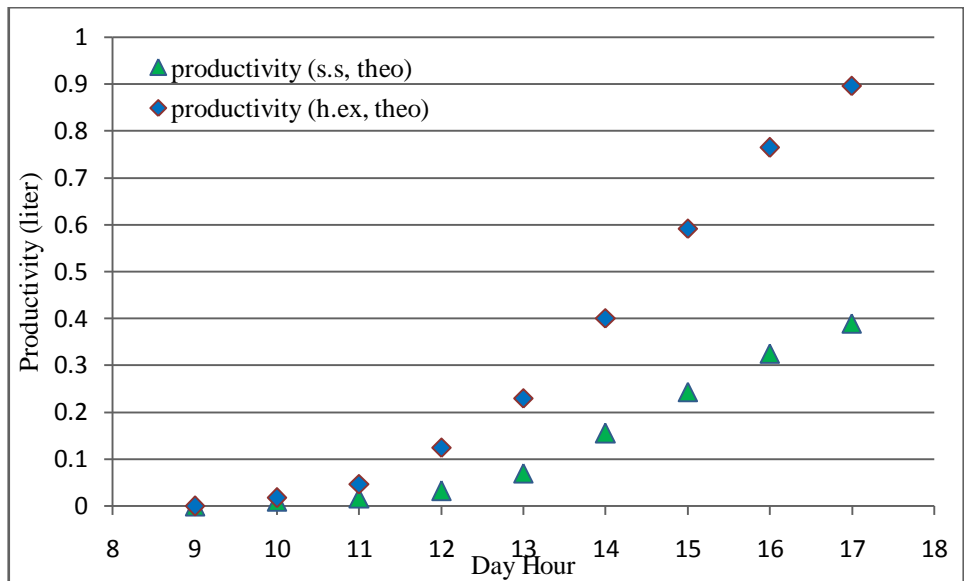


Fig .5.32: Theoretical accumulated productivityfor ETC and standalone solar still, (March20, 2016)

5.4. Conclusion

Based on results of experimental and theoretical investigations, it could be concluded that:

- Solar energy distilling process are relatively inexpensive, low-technology systems, especially useful where the need for small plants.
- Solar distillation exhibits a considerable economic advantage over other salt water distillation processes, because of cost-free energy.
- Using FPC with solar still had a negative effect on its productivity in both open and closed loop system.
- The flat plate collector is effective in the condition with low solar intensity and low temperature.
- Productivity of solar still coupled with ETC in an open system is higher than the productivity of standalone solar still only for the first three hours that is due to consumption of stored hot water stored in the tank of ETC therefore, the daily productivity becomes less than that of the standalone solar still.
- Using ETC with solar still had a positive effect on the productivity in closed loop system and negative effect in case of open loop system.
- It was found that the productivity of the coupled still becomes 2.6 higher than the standalone solar still when the system running for 7 hour and the productivity is increased by 2.75 when the system running for 12 hours.

- The overall daily productivity of the proposed still under practical conditions assuming poorness of construction and operation skills is predicted to be about $6.45\text{kg/m}^2/12\text{ hour}$ and $5.55\text{kg/m}^2/7\text{ hour}$.

- The present still design leads to relatively higher distilled water output due to higher basin water temperature. Producing fresh water by a solar still with its simplicity would be one of the best solutions to supply fresh water to small isolated communities with no technical facilities.

- Due to good agreement of the theoretical analysis (Matlab program) with the experimental results we can predict the productivity of solar still and investigate the performance of solar still into large scale under the different working condition and time and different locations.

References

- [1] <http://www.savewater-sunna.com>
- [2] Ali M. El-Nashar, The economic feasibility of small solar MED seawater desalination plants for remote arid areas, Desalination 134 (2001) 173–186.
- [3] <http://www.whyfiles.org>
- [4] Hisham M. El-Kady, F.El-Shibini, Desalination in Egypt and the future application in supplementary irrigation, Desalination 136 (2001) 63-72.(3)
- [5] Azza Hafez, Samir El-Manharawy, Economics of seawater RO desalination in the Red Sea region, Egypt. Part 1. A case study, Desalination 153 (2002) 335-347.
- [6] www.onlyzerocarbon.org
- [7] Douglas Foy, Energy& Air Pollution, American Gas Association ad, 1991.
- [8] Mohamed A. Eltawil, Zhao Zhengming, Liqiang Yuan. A review of renewable energy technologies integrated with desalination systems. Renewable and Sustainable Energy Reviews 13 (2009) 2245–2262.
- [9] Mansour A .Mohammad et al ,Study of water desalination by solar energy using multi-stage flash msf process
- [10] <http://www.oksolar.com>
- [11] Soteris A. Kalogirou, Solar thermal collectors and applications, Progress in Energy and Combustion Science 30 (2004) 231–295.

- [12] Moh'd S. Abu-Jabal, I. Kamiya, Y. Narasaki, Proving test for a solar-powered desalination system in Palestine, *Desalination* 137 (2001) 1–6.
- [13] Kyritsis S. Proceedings of the Mediterranean Conference on Renewable Energy Sources for Water Production. European Commission, EURORED Network, CRES, EDS, Santorini, Greece; 10–12 June, 1996. p. 265–70.
- [14] Valverde Muela V. Planta Desaladora con Energia Solar de Arinaga (Las Palmas de Gran Canaria). Departamento de Investigacion Nuevas Fuentes. Centro de Estudios de la Energia; April, 1982.
- [15] Palma F. Seminar on new technologies for the use of renewable energies in water desalination, Athens 1991. Commission of the European Communities, DG XVII for Energy, CRES (Centre for Renewable Energy Sources) 1991.
- [16] Manjares R, Galvan M. Solar multistage flash evaporation (SMSF) as a solar energy application on desalination processes. Description of one demonstration project. *Desalination* 1979; 31(1–3):545–54.
- [17] Delyannis EE. Status of solar assisted desalination: a review, *Desalination* 1987; 67:3–19.
- [18] Hanafi A. Design and performance of solar MSF desalination system. *Desalination* 1991; 82 (1–3): 165–74.
- [19] Banat F, Jwaied N. Economic evaluation of desalination by small-scale autonomous solar-powered membrane distillation units. *Desalination* 2008; 220:566–73.
- [20] Duffle JA, Beckman WA. Solar engineering of thermal process. New York, USA: Wiley; 1991.

- [21] Sukhamte SP. Solar energy: principle of thermal collection and storage. New Delhi: Tata Mc Grawth-Hill; 1987.
- [22] www.researchgate.net
- [23] G.N. Tiwari, S.B. Sharma and M.S. Sodha, Energy Conser. Mgmt., 24(2) (1984) 155.
- [24] www.alternative-energy-tutorial.com
- [25] Moustafa M. Elsayed, Ibrahim S. Taha, Jaffar A. Sabbagh, Design of solar thermal systems, Scientific publishing center King Abdulaziz University, Jeddah, 57-61 (1994).
- [26] Hilal Al-Hinai, MS. Al-Nassri, B.A. Jubran. Parametric investigation of a double-effect solar still in comparison with a single-effect solar still, Desalination 150 (2002) 75-83.
- [27] Y.P. Yadav and G.N. Tiwafi, Energy Conser. Mgmt, 27(3) (1987) 327.
- [28] Abdul Jabbar N. Khalifa, Ahmad M. Hamood. Effect of insulation thickness on the productivity of basin type solar stills: An experimental verification under local climate. Energy Conversion and Management 50 (2009) 2457–2461.
- [29] S.M. Elsherbiny and H.E.S. Fath, Int. J. Solar Energy, 16 (1995) 277.
- [30] M. M. Elsayed, I. S. Taha and J. A. Sabbagh, Design of Solar Thermal Systems, Scientific Publishing Center, King Abdulaziz University, Saudi Arabia, 986
- [31] Hiroshi Tanaka, Yasuhito Nakatake, Factors influencing the productivity of multiple-effect diffusion-type solar still coupled with a flat plate reflector, Desalination 186 (2005) 299–310

- [32] Ajay Kumar Kaviti ,Akhilesh Yadav, Amit Shukla.Inclined solar still designs: A review,Renewable and Sustainable Energy Reviews Nov 2015
- [33] Moustafa M. Elsayed, Ibrahim S. Taha, Jaffar A. Sabbagh, Design of solar thermal systems, Scientific publishing center King Abdulaziz University, Jeddah, 57-61 (1994).
- [34] S.M.A. Moustafa, G.H. Brusewitz and D.M. Farmer, Solar Energy, 22 (1979) 141.
- [35] Moustafa M. Elsayed, Ibrahim S. Taha, Jaffar A. Sabbagh, Design of solar thermal systems, Scientific publishing center King Abdulaziz University, Jeddah, 57-61 (1994).
- [36] G.N. Tiwari, S.B. Sharma and M.S. Sodha, Energy Conser. Mgmt., 24(2) (1984) 155.(24)=AayushKaushal , Varun , Solar stills: A review , Renewable and Sustainable Energy Reviews 14 (2010) 446–453
- [37] Ajay Kumar Kaviti ,Akhilesh Yadav, Amit Shukla.Inclined solar still designs: A review,Renewable and Sustainable Energy Reviews Nov 2015
- [38] G.N. Tiwari and Y.P. Yadav, Energy Conser. Mgmt., 27(14) (1985) 327.
- [39] A.N. Minasian and A.A. Al-Kara ghoui, Energy Conser. Mgmt. 36(3) (1995) 2131.
- [40] T. Arunkumar, R. Jayaprakash, D. Denkenberger, AmimulAhsan, M.S. Okundamiya, Sanjay kumar, Hiroshi Tanaka, H.Ş. Aybar, An experimental study on a hemispherical solar still , Desalination 286 (2012) 342–348.

- [41] A.A. Kabeel, Performance of solar still with a concave wick evaporation surface, *Energy* 34 (2009) 1504–1509.
- [42] S.A. Lawrence, S.P. Gupta and G.N. Tiwari, *Int. J. Solar Energy*, 6 (1988) 291.
- [43] Ali A. Badran, Ahmad A. Al-Hallaq, Imad A. Eyal Salman, Mohammad Z. Odat, A solar still augmented with a flat-plate collector, *Desalination* 172 (2005) 227–234
- [44] Delyannis E. Historic Background of Desalination and Renewable Energies. *J Solar Energy Elsevier*. 2003; 75: 357–366.
- [45] Abdul Jabbar N. Khalifa, Ahmad M. Hamood. Effect of insulation thickness on the productivity of basin type solar stills: An experimental verification 79 under local climate. *Energy Conversion and Management* 50 (2009) 2457–2461.
- [46] A. Safwat Nafey, M. Abdelkader, A. Abdelmotalip, A.A. Mabrouk. Enhancement of solar still productivity using floating perforated black plate. *Energy Conversion and Management* 43 (2002) 937–946.
- [47] Hiroshi Tanaka, A theoretical analysis of basin type solar still with flat plate external bottom reflector, *Desalination* 279 (2011) 243–251
- [48] Akash, BA, Mohsen, MN, Nayfeh, W: Experimental study of the basin type solar still under local climatic conditions. *Energ. Convers. Manage.* 41, 883–890 (2000)
- [49] T.V. Arjunan, H. S. Aybar, N. Nedunchezian and M. Sakthivel, (2009), ‘Effect of Blue Metal Stones on the Performance of a Conventional Solar Still’, *Journal of Convergence in Engineering, Technology and Science*, 1, pp 17–22.

- [50] AK Tiwari, GN Tiwari (2006) Effect of water depths on heat and mass transfer in a passive solar still: in summer climatic condition. *Desalination* 195, 78-94.
- [51] Mahmoud. I.M. Shatat, K. Mahkamov. Determination of rational design parameters of a multi-stage solar water desalination still using transient mathematical modeling. *Renewable Energy* 35 (2010) 52–61.
- [52] Sodha MS, Kumar Asvini, Tiwari GN. Utilization of waste hot water for distillation. *Desalination* 1981;37:325–42.
- [53] V. Gnaneshwar and N. Nimlakhandan (2010), ‘Sustainable desalination using solar energy’, *Energy conversion & management*, 51, pp. 2245-2251.
- [54] Al-Kharabsheh S, Goswami D Y. Experimental study of an innovative solarwater desalination system utilizing a passive vacuum technique. *Solar Energy* 2003; 75(5): 395-401.
- [55] Tiwari GN, DimriVimal, Singh Usha, ChelAravind, SarkarBikash. Comparative thermal performance evaluation of an active solar distillationsystem. *International Journal of Energy Research* 2007;31:1465–82.
- [56] M.A.mohamed et al, Experimental and financial investigation of a symmetrical solar stills with different insulation, 0306-2619(95)00043-7
- [57] J.S. Gawande , L.B. Bhuyar, Effect of Design, Climatic and Operational Parameters on the Performance of Stepped Type Solar Still, DES-D-13-01342.

- [58] Moustafa M. Elsayed, Ibrahim S. Taha, Jaffar A. Sabbagh, Design of solar thermal systems, Scientific publishing center King Abdulaziz University, Jeddah, 57-61 (1994).
- [59] J.S. Gawande et al, Effect of design, climatic and operational parameters on the performance of stepped type solar still, DES-D-13-01342.
- [60] V. Velmurugan, S. S. Kumaran, V.N. Prabhu, K. Srithar, Productivity enhancement of stepped solar still – Performance analysis, Thermal Science, 12, (2008), 153-163.

APPENDIX A

GOVERNING EQUATION

The governing equations applied to a solar still can be summarized as following:

- Heat analysis in a passive solar still
- Heat analysis in an active solar still
- Overall thermal efficiency of solar still

▪ Internal heat transfer coefficients

Heat transfer occurs across the humid air inside the enclosure of the distillation unit by free convection which is caused by the action of buoyancy force due to density variation in the humid air. Density variation is caused by a temperature gradient in the humid air.

The convective heat transfer rate from water surface to condensing glass cover is given By:

$$q_{c,w-g} = h_{c,w-g}(T_w - T_g)W/m^2 \quad (1)$$

Where,

$h_{c,w-g}$ is convective heat transfer coefficient from water surface to condensing glass cover. The convective heat transfer coefficient $h_{c,w-g}$ is calculated by using the non-dimensional Nusselt number as shown below:

$$Nu = h_{c,w-g} \frac{L_c}{K_a} = C(Gr.Pr)^n \quad (2)$$

Where, c and n are constants

In equation (2), non- dimensional numbers Gr and Pr are called Grashoff number and Prandtl numbers respectively. These numbers are expressed as [59]:

$$Gr = \frac{d_e g \beta \rho \Delta T}{\mu} (3)$$

$$Pr = \frac{\mu C_{p_w}}{k_a} (4)$$

Where,

$$\Delta T = (T_w - T_g) + \frac{(P_w - P_g)(T_w + 273.15)}{268.9 \times 10^3 - P_w} \text{ } ^\circ\text{C} \quad (5)$$

Equation (2) can be rewritten as,

$$h_{c,w-g} = \frac{k_a}{d_e} \cdot C \cdot (Gr \cdot Pr)^n \text{ W/m}^2 \cdot \text{K} (6)$$

$$h_{c,w-g} = \frac{k_a}{d_e} \cdot C \cdot (Ra)^n \text{ W/m}^2 \cdot \text{K} (7)$$

Where,

$Ra = Gr \cdot Pr$ is the Rayleigh number.

Malik *et al.*, [60] assumed that water vapour obeys the perfect gas equation and have given the expression for evaporative heat transfer rate as:

$$q_{e,w-g} = h_{e,w-g} (T_w - T_g) \text{ W/m}^2 (8)$$

Where

$h_{e,w-g}$ is the evaporative heat transfer coefficient between water surface and condensing glass cover and expressed as

$$h_{e,w-g} = 0.01623 \cdot h_{c,w-g} \frac{(P_w - P_g)}{(T_w - T_g)} \text{ W/m}^2 \cdot \text{K}$$

$$P_w = e^{(25.317-5144/T_w)}$$

$$P_g = e^{(25.317-5144/T_g)}$$

Substituting the value of $h_{e,w-g}$ in equation (6) above, we get

$$q_{e,w-g} = 0.01623 \cdot h_{c,w-g} (P_w - P_g) \text{ W/m}^2 \text{ (9)}$$

Substituting the value of $h_{c,w-g}$ in the above equation, we get

$$q_{e,w-g} = 0.01623 \cdot \frac{k_a}{d_e} \cdot (P_w - P_{gi}) \cdot C \cdot (Ra)^n \text{ W/m}^2 \text{ (10)}$$

By knowing the evaporative heat transfer rate; mass of the water distilled can be derive by the following equation:

$$\dot{m}_{ew} = \frac{q_{e,w-g} A_w}{L} \text{ (11)}$$

$$\dot{m}_{ew} = 0.01623 \cdot \frac{k_a}{d_e} \cdot (P_w - P_g) \cdot C \cdot (Ra)^n \cdot \frac{1}{L} \cdot A_w \text{ (12)}$$

$$\dot{m}_{ew} = R \cdot C \cdot (Ra)^n \text{ (13)}$$

$$\frac{\dot{m}_{ew}}{R} = C \cdot (Ra)^n \text{ (14)}$$

$$R = 0.01623 \cdot \frac{k_a}{d_e} \cdot (P_w - P_g) \cdot \frac{1}{L} \cdot A_w$$

In equation (14), there are two unknown parameters C and n. They are determined by regression analysis using experimental values of distillation yield (\dot{m}_{ew}), saline water temperature in the basin (T_w), glass cover temperature at the inner surface (T_{gi}).

Equation (14) can be rewritten in the following form:

$$Y = aX^b \text{ (15)}$$

Where,

$$Y' = \frac{\dot{m}_{ew}}{R}; X=Ra; a = c; b = n$$

Equation (15) can be reduced to a linear equation by taking log on both the sides:

$$\ln(Y) = \ln(a) + b\ln(X) \quad (16)$$

$$Y' = a' + b'X' \quad (17)$$

$$Y' = \ln(Y); a' = \ln(a); b' = b; X' = \ln(X) \quad (18)$$

Coefficients a' and b' are calculated using regression analysis. The expressions for a' and b' are given by:

$$b' = \frac{N(\sum X'Y') - (\sum X')(\sum Y')}{N(\sum X'^2) - (\sum X')^2} \quad (19 a)$$

$$a' = \frac{\sum Y'}{N} - b' \frac{\sum X'}{N} \quad (19 b)$$

Where,

N is the number of experimental observations.

Knowing a' and b' from equation (17), the value of C and n can be obtained by the following expressions:

$$C = e^{a'} \text{ and } n = b'$$

Once the values of C and n are known, the experimental data can be used to obtain the internal heat and mass transfer coefficients for the solar stills are evaluated. Equation (2) can be used to obtain the convective heat transfer coefficient $h_{c,w-g}$ [46], by using the values of $C=0.075$ and $n = 1/3$, gave following expression for $h_{c,w-g}$, valid for a mean operating temperature range of approximately 50°C.

$$h_{c,w-g} = 0.884[(T_w - T_g) + \frac{(P_w - P_g)(T_w + 273.15)}{(268.9 \times 10^3 - T_w)}]^{1/3} \text{W/m}^2 \cdot \text{K} \quad (20)$$

$$h_{e,w-g} = 0.01623 \cdot h_{c,w-g} \frac{(P_w - P_g)}{(T_w - T_g)} \text{W/m}^2 \cdot \text{K} \quad (21)$$

$$q_{e,w-g} = h_{e,w-g} (T_w - T_g) \text{W/m}^2 \quad (22)$$

The irradiative heat transfer coefficient between the water surface and condensing glass cover is given by is given by following equation:

$$h_{r,w-g} = \epsilon_{eff} \sigma [(T_w + 273)^2 + (T_g + 273)^2] (T_w + T_g + 546)$$

$$\text{W/m}^2 \cdot \text{K} \quad (23)$$

Where,

$$\sigma = 5.669 \times 10^{-8} \text{W/m}^2 \text{K}^2$$

$$\epsilon_{eff} = \frac{1}{\frac{1}{\epsilon_w} + \frac{1}{\epsilon_g} - 1}$$

ϵ_g and ϵ_w are emissivity of basin water and glass cover and are given by

$$\epsilon_g = \epsilon_w = 0.9$$

$$q_{r,w-g} = h_{r,w-g} (T_w - T_g) \text{W/m}^2 \quad (24)$$

APPENDIX B

MATHEMATICAL CODE

```
Clear
clc
tg(1)=input('initial glass temperature(c)=');
Tw (1) =input ('initial water temperature(c) =');
%Is=input ('solar intensity (w/m2) =');
%tas=input ('ambient temperature(c) =');
%Is= [480 630 770 716 595 519 370 170 110 50] ;('solar intensity (w/m2) =');
%Is= [510 620 790 750 615 541 391 200 100 56] ;('solar intensity (w/m2) =');
%Is= [490 630 725 640 605 580 470 320 161 100] ;('solar intensity (w/m2)=');
%Is= [570 658 759 766 725 660 507 376 207 60] ;('solar intensity (w/m2) =');
Is= [570 650 700 750 742 659 518 368 205 50] ;('solar intensity (w/m2) =');
%Is= [470 400 388 540 616 490 540 230 190 68] ;('solar intensity (w/m2) =');
%Is= [770 761 711 581 463 326 164] ;('solar intensity (w/m2) =');
%Is= [758 744 655 540 402 257 79] ;('solar intensity(w/m2)=');
%Is= [570 650 711 685 622 581 463 326 164 70 0 0 0];
('solar intensity (w/m2) =');
%Is= [838 927 933 930] ;('solar intensity (w/m2) =');
%tas= [31.5 35 40 37.5 36.5 36 35.8 35 33.7 32];
('ambient temperature(c) =');
%tas=[32 34 36 38.4 35.5 34.6 32.2 31 29.2 28] ;('ambient temperature(c)=');
% tas= [34 36.5 39.2 42.5 38.5 36.2 35.9 34.5 33.5 32.1 31.2 29.2 28];
('ambient temperature(c) =');
tas=[35 37.5 41.3 46.5 40.1 39.2 38.9 35.1 34.5 33];
('ambient temperature(c) =');
%tas= [32 34 36 38.4 35.5 34.6 32.2 31 29.2 28] ;('ambient temperature(c)=');
%tas= [41.4 41 40.5 39.8 39.2 38 37] ;('ambient temperature(c) =');
sumwater(1)=0;('intial distilled water (kg)=');
disl(1)=0;
%Mex=input ('Mex=');
% touthex=input ('output temperature for heat exchanger in each hour(c) =');
% tinhex=input ('input temperature for heat exchanger in each hour(c) =');
% touthex=[40 43 45 48.9 49 42 39.1 38.1 34.9 33 ];
('output temperature for heat exchanger in each hour(c) =');
% tinhex= [41 45 47.5 49.7 50 42.1 39.5 38.2 36 35];
('input temperature for heat exchanger in each hour(c) =');
t= [1 2 3 4 5 6 7 8 9 10] ;('time interval=');
%t= [1 2 3 4 5 6 7 8 9 10 11 12 13] ;('time interval=');
%t= [1 2 3 4 5 6 7] ;('time interval=');
for N=1:10;('TIME LOOP');
tbs (1)=Tw(1);('initial basin temperature(c)=');
```

```

TG=tg (N) ;('glass temperature in each hour(c) =');
tw= Tw(N);('water temperature in each hour(c)=');
ta=tas(N);('ambint temperature in each hour(c)=');
% va=vs(N);('velocity of air(km/hr))=');
tb=tbs(N);('basin temperature in each hour(c)=');
I=Is(N) ;('solar intensity in each hour(c)=');
% |-----|
% | CONSTANT VALUES |
% |-----|
for W=1:1000% iteration error loop
c_s=0.11*10^6 ;(' J/m2.c');
ebsilon_g=0.89;
% vs= [20 20 20 20 20 20 20 20 20 20];
va=10;('velocity of air((km/hr))=');
taw_g=0.89;
tsky=ta-6;
coss=0.939;
a=5.61 ;
b=1.09 ;
n=1 ;
Mw=0.00833;('mass of water into solar still(kg/s.m2)=');
Mc=0.00833;('mass of water c collector(kg/s.m2)=');
alfa_water=0.8;('absorbtivity of water=');
alfa_glass=0.1;('absorbtivity of glass=');
alfa_basin=0.8;('absobtivity of basin=');
% L=800;('latent haet of vaporizatonof water(MJ/kg)=');
Aw=1;('area of water(m2)=');
Ag=1;('area of glass(m2)=');
A_hex=1;('area of heat exchanger(m2)=');
A_b=1;('area of basin(m2)=');
h_hex=5;('overall heat coefficient for heat exchanger(w/m2.c)=');
h_b=5;('overall heat coefficient for basin(w/m2.c)=');
A_c=2;('area of collector (m2)=');
cp_w=4190;('average specific heat coefficient of water(J/kg.c)=');
% |-----|
% |EQUATION OF MATHMATICAL MODEL |
% |-----|
f1=25.317-(5144/(TG+273.15));
f2=25.317-(5144/(tw+273.15));
pg=exp (f1) ;('glass pressure (N/m2) =');
%fprintf( 'pg=%d',pg);
pw=exp(f2);('water pressure(N/m2)=');
%fprintf( 'pw=%d',pw);

```

```

dt=tw-TG;
%-----
hc_water_glass(N)=0.884*((tw-TG)+(((pw-pg)*(tw+273.15))/(265.9e+3-
pw)))^(1/3);('convective heat transfer coefficient from water surface to glass
(W/m2.C1)=');
fprintf('hc_water_glass=%d',hc_water_glass);
fprintf('\n');
%-----
qc_haet_convection(N)=(hc_water_glass(N)*Aw*(tw-TG));('convective heat
transfer (w/m2)=');
fprintf('qc_haet_convection=%d',qc_haet_convection);
fprintf('\n');
%-----
sigma=5.6e-8;('Stefan-Boltzmann constant (W/m2 K4)=');
Ibsilon=0.82;('emissivity constant=');
hr_water_glass(N)=(Ibsilon*sigma)*((tw+273)^2+(TG+273)^2)*(tw+TG+54;
('Radiative heat transfer coefficient from water surface to glass (W/m2.C1)=');
fprintf('hr_water_glass=%d',hr_water_glass);
fprintf('\n');
%-----
qr_haet_radiation(N)=(hr_water_glass(N)*Aw*(tw-TG));
('radiative heat transfer (w/m2)=');
fprintf('qr_haet_radiation=%d',qr_haet_radiation);
fprintf('\n');
%-----
he_water_glass(N)=0.01623*hc_water_glass(N)*((pw-pg)/(tw-TG));
('evaporative heat transfer coefficient from water surface to glas(W/m2.C1)=');
fprintf('he_water_glass=%d',he_water_glass);
fprintf('\n');
%-----
qe_haet_evaporation(N)=(he_water_glass(N)*Aw*(tw-TG));
('evaporative heat transfer (w/m2)=');
fprintf('qe_haet_evaporation=%d',qe_haet_evaporation);
fprintf('\n');
%-----
% t_hex(N)=(touthex(N)+tinhex(N))/2;
('avarage temp into heat exchanger(c)=');
% q_losses(N)=A_hex*h_hex*(t_hex(N)-ta);
('heat losses from heat exchanger(w/m2)');
% Delta_T(N)=(touthex(N)-tinhex(N));
('(differance temp between input and output into heat exchanger(c))=');
% q_convective_hex_b=Mex*cp_w*Delta_T(N)-q_losses(N);
('convective heat transfer from heat exchanger to basin (w/m2)=');

```

```

% fprintf('q_convective_hex_b=%d',q_convective_hex_b);
% fprintf('\n');
%-----
% qc_b_w=(I*(alfa_water)*(alfa_glass)*(alfa_basin))-(h_b*A_b*(tb-
ta))+(q_convective_hex_b);
('convective heat transfer from basin to water (w/m2)=');
% %qe_haet_evaporation2=qc_b_w+(I*alfa_water*(1-alfa_glass))-
qr_haet_radiation-qc_haet_convection;
% qe_haet_evaporation2=qe_haet_evaporation+q_convective_hex_b;
%-----
L=(1000*(3161.5)-(2.4074*(tw+273)));
mass_water_vapour_i(N)=((qe_haet_evaporation(N))*0.33*3600)/L;
('distilled water(kg/s.m2)=');
fprintf(' mass_water_vapour_=%d',mass_water_vapour_i);
fprintf('\n');
eta_solar_still(N)=((qe_haet_evaporation(N))*0.33)/(I);
fprintf(' eta_solar_still(N)=%d',eta_solar_still(N));
fprintf('\n');
%-----
%|-----|
%| EQUATION OF BALANCE |
%|-----|
q_b(N)=h_b*A_b*(tw-tb);
% dis(N)=(3.125e-7*I)-(3.438e-5);
% disl(N+1)=disl(N)+dis(N);
h_g_a(N)=(a+((b*(va)^n)));
('heat transfer to ambient from equation mc adams 1956 in dr mosta-
fa(w/m2)=');
fg_s=(1/2*(1+cos));
f_sky=(1/((1/fg_s)+((1-ebpsilon_g)/ebpsilon_g)));
d=(h_g_a(N)*Ag*(TG-tsky));
s=(f_sky*sigma*((TG+273)^4-(tsky+273)^4));
q_g_a1(N)=(d+s);
('heat transfer balance in the glass surface to ambient (w/m2)=');
q_g_a2(N)=(qr_haet_radiation(N)+qe_haet_evaporation(N)+qc_haet_convecti
on(N)+(alfa_glass*Ag*I));
('heat transfer balance in the glass surface to ambient (w/m2)=');
w=((alfa_glass*Ag*I)+(I*alfa_water*Ag*taw_g));
% w2=((alfa_glass*I)+(I*alfa_water*taw_g)+(q_convective_hex_b));
v=(q_g_a2(N)+q_b(N));
% v2=(q_g_a1+q_b+q_f+q_losses);
z=w-v;
% z2=w2-v2;

```

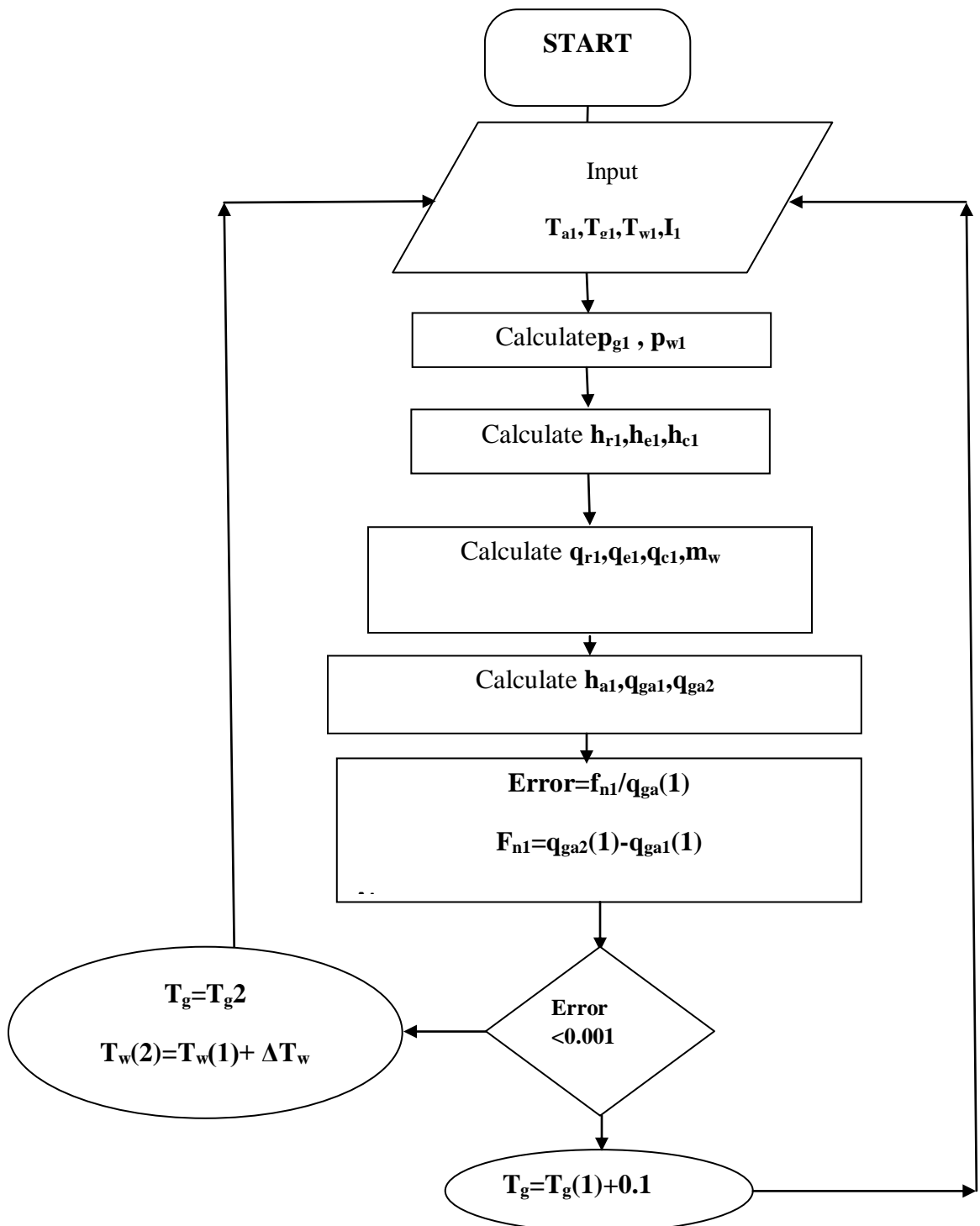
```

delta_tw=((z*3600)/c_s);
fprintf( 'delta_tw=%d',delta_tw);
fprintf('\n');
error=((q_g_a2(N)-q_g_a1(N))/q_g_a1(N));('error');
fprintf( 'error=%d',error);
fprintf('\n');
    if error >=0.0001
        TG = TG + 0.5;
        Tw (N+1) = Tw (N) + (delta_tw);
        tbs (N+1)=tbs (N) + (delta_tw);
    else
        TG = TG - 0.5;
        tbs (N+1) = tbs (N) - (delta_tw);
        tg (N+1) = TG;
        Tw (N+1) = Tw (N) +(delta_tw);
        sumwater (N+1) = sumwater (N) + mass_water_vapour_i(N);
    end
end%end loop iterationl
end%end loop time
% plot(t,Tw,t,tg);
% title('')
% xlabel('time')
% ylabel('hr.water.glass')
%plot(t,tg);
% plot(t,mass_water_vapour_i);
%plot(t, distilled_water);
% plot(t, eta_solar_still);
% plot(t,qe_haet_evaporation,t,qr_haet_radiation,t,qc_haet_convection)
% plot(t,qr_haet_radiation);
% plot(t,qc_haet_convection);
% plot(t,Is);

%-----

```

FLOW CHART



APPENDIX C

Solar still coupled with ETC and standalone theoretical and experimental results are tabulated herein under in table C.1 and C.2.

Table C.1: Numerical and experimental results (08/08/2014)

date	time	I	Ta	Tw (s.s, theo)	Tw (s.s, exp)	Tg (s.s,theo)	Tg (s.s,exp)	Productivity (s.s, theo)	Productivity (s.s, exp)
08/08/2014	12	770	41.4	63	63	47	47	0	0
08/08/2014	13	761	41	69.316	67.5	54	55	0.104	0.1
08/08/2014	14	711	40.5	69.273	67	60	59.5	0.253	0.22
08/08/2014	15	581	39.8	66.203	63	59.5	57.7	0.410	0.38
08/08/2014	16	463	39.2	63.206	57.1	56.5	51	0.544	0.5
08/08/2014	17	326	38	60.108	51	53.5	47.5	0.659	0.6
08/08/2014	18	164	37	55.115	44	50	40.1	0.764	0.67

date	time	I	Ta	Tw (h.ex, theo)	Tw (h.ex, exp)	Tg (h.ex,theo)	Tg (h.ex,exp)	Produc tivity (h.ex,theo)	produc tivity (h.ex,ep)
08/08/2014	12	770	41.4	63.7	63	49	49	0	0
08/08/2014	13	761	41	86	72.60612	54	64	0.156484	0.15
08/08/2014	14	711	40.5	87	78.89203	63	65	0.41095	0.4
08/08/2014	15	581	39.8	84.5	79.96788	69.5	64	0.737352	0.7
08/08/2014	16	463	39.2	81.5	78.00423	70.5	63	1.076476	1
08/08/2014	17	326	38	80	71.81278	68	62	1.403938	1.35
08/08/2014	18	164	37	72.4	70.52214	61	59	1.698848	1.61

Table C.2: Numerical and experimental results (09/07/2014)

date	time	I	Ta	Tw (s.s, theo)	Tw (h.ex, exp)	Tg (s.s,theo)	Tg (s.s,exp)	Produc tivity (s.s, theo)	Produc tivity (s.s, exp)
09/07/2014	10	570	34	50	50	40	40	0	0
09/07/2014	11	650	36.5	55.36	57	40.5	41	0.058	0.05
09/07/2014	12	711	39.2	60.95	61	46	46	0.133	0.1
09/07/2014	13	685	42.5	65.47	66.5	51.5	49	0.233	0.2
09/07/2014	14	622	38.5	68.61	67	56.5	53	0.351	0.3
09/07/2014	15	581	36.2	65.276	63	58.5	56.7	0.509	0.45
09/07/2014	16	463	35.9	63.13	57.1	54.5	52	0.654	0.55
09/07/2014	17	326	34.5	58.95	51	52	46.5	0.789	0.6
09/07/2014	18	164	33.5	53.62	44	47.5	42.1	0.903	0.65
09/07/2014	19	70	32.1	47.95	40	42.5	39	0.987	0.68
09/07/2014	20	0	31.2	44.47	35	37.5	34	1.046	0.72
09/07/2014	21	0	29.2	41.77	31	34.5	30	1.093	0.77
09/07/2014	22	0	28	40.34	29	31.5	28	1.134	0.8

date	time	I	Ta	Tw (h.ex, theo)	Tw (h.ex, exp)	Tg (h.ex,theo)	Tg (h.ex,exp)	Produc tivity (h.ex,theo)	Product ivity (h.ex,exp)
09/07/2014	10	570	34	51	50	40.5	40.5	0	0
09/07/2014	11	650	36.5	63.65	57	41.5	49	0.13	0.1
09/07/2014	12	711	39.2	75.55	61	53	60	0.36	0.3
09/07/2014	13	685	42.5	75.98	66.5	65.5	66.5	0.66	0.6
09/07/2014	14	622	38.5	78.44	67	67	65	0.93	0.9
09/07/2014	15	581	36.2	72.98	63	68.5	64	1.252	1.2
09/07/2014	16	463	35.9	71.75	57.1	62	63	1.54	1.4
09/07/2014	17	326	34.5	71.35	51	61	62	1.83	1.6
09/07/2014	18	164	33.5	66.89	44	60	59	2.12	1.85
09/07/2014	19	70	32.1	58.16	40	54.5	53	2.37	2.01
09/07/2014	20	0	31.2	51.57	35	45.5	44	2.55	2.1
09/07/2014	21	0	29.2	41.38	31	39.5	37	2.65	2.2
09/07/2014	22	0	28	29.94	29	31.5	32	2.68	2.25

Solar still coupled with ETC and standalone theoretical results are tabulated herein under in table C.3 and C.4.

Table C.3: Numerical results (23/01/2016)

date	Time	I	T _a	T _w (s.s, theo)	T _w (h.ex, theo)	T _g (s.s,theo)	T _g (h.ex,theo)	Productivity (s.s,theo)	Productivity (h.ex,theo)
23/01/2014	9	90	12.5	13	13	7	7	0	0
23/01/2014	10	220	13	13.950513	14.037952	8.5	8.5	0.0030583	0.0120788
23/01/2014	11	400	14.5	18.063603	19.866308	9.5	9.5	0.0062418	0.042341
23/01/2014	12	570	15.5	24.248229	29.941355	12	13	0.0123311	0.0869781
23/01/2014	13	430	15.2	33.439644	39.592114	16	18.5	0.0249818	0.1442964
23/01/2014	14	320	15	32.895454	37.985707	20	24	0.0613233	0.2077592
23/01/2014	15	210	14.5	29.848334	34.680688	19.5	22.5	0.0964929	0.2651748
23/01/2014	16	105	14	25.041771	30.739028	17	20	0.1250124	0.3122281
23/01/2014	17	40	13.7	19.403756	26.947313	14	17	0.1435603	0.3532027

Table C.4: Numerical results (20/03/2016)

date	time	I	T _a	T _w (s.s, theo)	T _w (h.ex, theo)	T _g (s.s,theo)	T _g (h.ex,theo)	productivity (s.s, theo)	productivity (h.ex, theo)
20/03/2014	9	150	21	25	25	18	18	0	0
20/03/2014	10	340	23	26.18544	25.71139	18.5	18.5	0.009816	0.017709
20/03/2014	11	510	25.5	32.25206	32.82898	21	20.5	0.017613	0.047432
20/03/2014	12	650	27	41.16609	47.76053	25.5	26	0.032876	0.125205
20/03/2014	13	600	26	50.76305	56.03894	31.5	36	0.0707	0.229997
20/03/2014	14	550	25.1	50.43796	59.80165	38	42.5	0.155539	0.400499
20/03/2014	15	400	24.3	48.92643	57.96924	37	45.5	0.243782	0.592191
20/03/2014	16	250	23.6	44.61564	50.96977	35.5	43	0.325405	0.764287
20/03/2014	17	100	22	38.99267	46.76853	31.5	36.5	0.389187	0.896547

دراسة تحليلية المياه المالحة بالطاقة الشمسية للتطبيقات المنزلية

ملخص الرسالة

الكثير من المناطق النائية في العالم مثل المناطق الساحلية الصحراوية في الشرق الأوسط ومنطقة البحر المتوسط يعانون من مشكلة نقص مياه الشرب , فمصر التي يفوق تعداد سكانها عن 90 مليون نسمة سوف تعاني مشكلة خطيرة في نقص المياه بحلول عام 2025. والجدير بالذكر ان استغلال مصادر المياه الطبيعية اقترانا مع الطلب المتزايد على استخدام الماء الى ارتفاع معدل البحث عن مصادر أخرى بديلة للماء الصالح للشرب.

ولقد احتل التقطير بالطاقة الشمسية الصدارة والاهتمام لعقود طويلة حيث انه يعتبر احدى الطرق النظيفة للحصول على الماء الصالح للشرب. وتعد مصر واحدة من أكثر الدول المشمسة في العالم. أما منطقة خليج السويس فهي واحدة من أكثر المناطق الحارة في مصر, ولذلك كان على رأس الأولويات استخدام تلك الطاقة الضخمة المتمركزة في منطقة خليج السويس في أجهزة تحليل المياه. وفي هذا العمل القائم تم تصميم وحدة تقطير بالطاقة الشمسية حيث يتم توصيلها بأنواع المختلفة من مجمعات الطاقة الشمسية ذات المعدلات المختلفة على سبيل المثال (السخان الشمسي الانبوبي - السخان الشمسي المسطح) وسيكون محل بحث وموضع اختبار في حالات عديدة خاصة في إنتاج كمية قليلة من الماء الصالح للشرب وفي استخدامات مجموعات محددة بعينها من البشر مثل (وحدات الجيش- البدو- الخ.....). هذا النظام تم تصميمه وأختباره في كلية هندسة وتعددين البترول بالسويس كذلك تم اختبار النظام في ظروف جوية مختلفة وتم عمل مقارنات لما تم الحصول عليه من نتائج بالنتائج المنشورة في أبحاث أخرى وكذلك النتائج النظرية التي تم الحصول عليها باستخدام النموذج الرياضي.

وقد تم اختبار نظام التقطير الشمسي في حالة اتصاله بالسخان الشمسي المسطح وعمل مقارنة النتائج لوحدة التقطير على حده والنتائج بعد توصيلها بالسخان . وقد وجد أن إنتاجية وحدة التقطير الشمسي 2.28 لتر/ 2م / 10 ساعة في حين أن الإنتاجية بعد توصيل الوحدة بالسخان الشمسي المسطح كانت 1.56 لتر / 2م / 10 ساعة. يمكن التأكيد على أن توصيل السخان الشمسي المسطح بوحدة التقطير الشمسي غير فعال في حالة الكثافة الشمسية المرتفعة بينما يمكن استخدامه في حالة كثافة الطاقة الشمسية المنخفضة ودرجات الحرارة المنخفضة. ذلك نظرا لأن درجة الحرارة الناتجة من السخان الشمسي المسطح أقل من درجة حرارة الماء في الحوض أسفل وحدة التقطير. في المقابل ، تشير

النتائج إلى أن إنتاجية وحدة التقطير الشمسى يمكن أن تعزى فى حالة توصيل الوحدة بالسخان الشمسى ذات الأنابيب المفرغة لتكون 6.45 لتر/ م²/ 10 ساعة.

تم عمل مقارنة بين النتائج النظرية و النتائج التجريبية, المقارنه أظهرت توافق مقبول بين كلا منهما. النتائج النظرية التى تم الحصول عليها من نموذج نظري (برنامج ماتلاب) من خلال تغذية البرنامج ببيانات الطقس مثل الحرارة وسرعه ارياح والكثافة الشمسيه في شهريناير و شهرمارس. وجد أن الإنتاجية تتراوح بين 1.0 لتر/ م²/ يوم فى يناير إلى 3.0 لتر/ م²/ يوم فى م ارس فى محافظة السويس.



السويس جامعة
كلية هندسة البترول والتعدين
قسم العلوم الهندسية



دراسة تحليلية المياه المالحة بالطاقة الشمسية للتطبيقات المنزلية

رسالة مقدمة الى
قسم العلوم الهندسية

كجزء من متطلبات الحصول على درجة الماجستير
في
هندسة الطاقة
من

المهندس/ محمد عبد الفتاح ابو المجد

بكالوريوس الهندسة الميكانيكية-الكلية الفنية العسكرية

2007

لجنة فحص ومناقشة الرسالة

د/ حسين محمد سليمان
قسم الطاقة الشمسية
المركز القومي للبحوث

د/ سامح عبد الواحد ندا
استاذ الهندسة الميكانيكية
كلية الهندسة
جامعة بنها

د/ هاني محمد الجوهري
قسم العلوم الهندسية
كلية هندسة البترول والتعدين
جامعة السويس

د/ احمد صفوت محمد
قسم العلوم الهندسية
كلية هندسة البترول والتعدين
جامعة السويس

السويس

2016



جامعة السويس
كلية هندسة البترول والتعدين
قسم العلوم الهندسية



دراسة تحليلية المياه المالحة بالطاقة الشمسية للتطبيقات المنزلية

رسالة مقدمة الى
قسم العلوم الهندسية
كجزء من متطلبات الحصول على درجة الماجستير

فى

هندسة الطاقة

من

المهندس/ محمد عبد الفتاح ابو المجد

بكالوريوس الهندسة الميكانيكية- الكلية الفنية العسكرية

2007

تحت اشراف

د/هانى محمد الجوهري
قسم العلوم الهندسية
لكلية هندسة البترول والتعدين
جامعة السويس

د/حسين محمد سليمان
قسم الطاقة الشمسية
المركز القومى للبحوث

السويس

2016